Journal of *Marine Science and Engineering*

MDPI

Article

Dynamic Response of Deep-Sea Trawl System during Towing Process

Dapeng Zhang [1], Bowen Zhao [2,*], Keqiang Zhu [3] and Haoyu Jiang [4]

[1] Ship and Maritime College, Guangdong Ocean University, Zhanjiang 524088, China
[2] Ocean College, Zhejiang University, Zhoushan 316000, China
[3] Faculty of Maritime and Transportation, Ningbo University, Ningbo 315211, China
[4] School of Electronics and Information Engineering, Guangdong Ocean University, Zhanjiang 316021, China
* Correspondence: zju_zhbw@zju.edu.cn

Abstract: The trawl system plays an irreplaceable role in deep-sea fishing. In the towing process of the trawl system, many complex mechanical phenomena occurs, so it is necessary to analyze the dynamic response of the deep-sea trawl system during the towing process. In this paper, an equivalent mathematical model for predicating the movement of the ocean trawl system is established based on the equivalent net theory. In the proposed method, the lumped mass method is used to simulate the towed cable and some lines with hydrodynamic characteristics are used to simulate the fishing net. The effects of towing speeds on the dynamic characteristics of a rigid truss trawl system and a flexible trawl system during straight-line towing and rotation towing are studied. The results show that it is possible to simulate trawl motion, and the trawling process is well-presented using this equivalent mathematical model. The disadvantage of this method is also obvious, that is, it cannot simulate trawls with a large number of meshes because the proliferation of mesh numbers can lead to difficult computational convergence. The results also demonstrate that during straight-line towing, the higher the speed, the greater the tension of the cable. Due to the rigid truss, the shape of the rigid truss trawl under different towing speeds is not much different, while the shape of the flexible trawl system changes greatly. During rotating towing, the tension of the cable changes abruptly in the initial stage, and then fluctuates periodically in the time domain. With the increase of towing speed, the overall outward floating distance of the trawl increases gradually. This study has a certain reference and guiding role for deep-sea fishing operations.

Keywords: dynamic response; towing process; rigid truss trawl system; flexible trawl system; lumped mass method

Citation: Zhang, D.; Zhao, B.; Zhu, K.; Jiang, H. Dynamic Response of Deep-Sea Trawl System during Towing Process. *J. Mar. Sci. Eng.* **2023**, *11*, 145. https://doi.org/10.3390/jmse11010145

Academic Editor: Spyros A. Mavrakos

Received: 1 December 2022
Revised: 31 December 2022
Accepted: 4 January 2023
Published: 7 January 2023

1. Introduction

The deep sea is abundant in fish resources. All types of fish are high in protein, and the fish flesh of marine fish is high in nutrition and easy to digest and absorb, making it an important complement for human consumption [1,2]. Fish may be rescued and processed from the water using various technology. The trawl mechanism is crucial in deep-sea fish mining. There are two varieties. The first is the fishery trawl system, which travels with the fishing boat [3]. The trawl is normally mounted on the fishing boat's stern or side.

After locating the shoal of fish, the fishing boat chases or intercepts the fish school using a series of maneuvers such as straight sailing acceleration and immediate turning to catch the fish school with the back trawl. The alternative option is either a single deep-water cage or a vast marine ranch made up of multiple enormous cages. For large-scale deep-sea aquaculture, this system often requires trawlers to pull it to the planned sea region, anchor and fix the system in the relevant sea area, and then place the fry in the cage or marine ranch in the predetermined sea area. It is important to study the towing process of a trawl system since it involves several complicated mechanical phenomena.

So far, many researchers have studied the dynamic behavior and characteristics of the trawl system, with different types of approaches [4–7]. Trawl system performance studies date back to the 1980s. Wileman and Hansen [8] carried out a series of flume tank experiments with model nets to evaluate the effect on net drag of a reduced netting twine area using larger meshes, thinner twines, and knotless nettings in different parts of the trawl. Somerton et al. [9] studied the escape of fish under the ground rope and the effect of sweep line on a trawl on gathering fish. Priour [10] developed a finite element method for simulating flexible structures made of nettings, cables, and bars, such as fishing gear and fish farming cage, which focused on a specific triangular element devoted to net modeling. Mulvany et al. [11] estimated the hydrodynamic forces on trawl doors using computational fluid dynamics (CFD) analysis by solving the Navier–Stokes equations with a finite element method. Kristiansen and Faltinsen [12] proposed and discussed a screen-type force model for the viscous hydrodynamic load on nets, assuming that the net is divided into several flat net panels.

Trawling is an effective and widely applicable fishing method. Trawling is inseparable from the trawler. The trawler operation can be divided into single-boat trawling and double-boat trawling. There is a towing process in these two trawler operations. In the simulations of trawler operation, the research mainly focuses on the physical modeling of the trawler warp and net. Khaled et al. [13,14] presented a mechanical model for trawls based on a finite element method, which was adapted to minimize the drag-to-mouth area ratio. They also explored the effect of cable length optimization on the ratio between the estimated trawl drag and the predicted catch efficiency. Lee et al. [15] proposed a novel trawl door with a trailing edge flap and a trawl door and evaluated the hydrodynamic characteristics at different flap angles through numerical analyses and experimentation. Thierry et al. [16,17] studied the drag of bottom trawl models constructed from traditional and new materials. The effect of twine stiffness, twine material, and mesh size on the hydrodynamic performance of bottom trawl and geometrical mouth shape were evaluated. You et al. [18] investigated the resistance performance and fluid-flow of a trawl plane netting at small angles of attack using hydrodynamic experiments and computational fluid dynamic (CFD). In CFD analysis, a finite volume method was used for solving Reynolds-Averaged Navier–Stokes equations. Wan et al. [19,20] studied the hydrodynamic performance of an Antarctic krill trawl system including trawler, cable, otter board, and trawl by means of numerical simulation combined with full-scale measurement at sea. The numerical model was established based on finite element method and the principle of minimum potential energy was employed to determine the equilibrium configuration of the trawl system in uniform current. Chen and Yao [21] modeled the trawl net and the flow field based on the lumped mass method and finite volume method to investigate the effect of the fluid-structures interaction on the trawl net's numerical model. Guan et al. [22] investigated the hydrodynamic performance of a new type of bottom trawl using numerical simulation and physical modeling methods. According to the literature, numerical simulation has become an important tool to study the hydrodynamic performance of the trawl system [23,24]. Mai The Vu and Hyeung-Sik Choi [25–30] provided valuable theories for establishing the mathematical model of dynamic coupled analysis of cable and trawl ships.

The structure of the trawl system is complex. Due to the flexibility of the nets in the streamer and cage systems, many strong nonlinear factors contribute to the calculation and design difficulties [31,32]. In addition, the flexibility of the net causes different spatial and mechanical properties in different engineering projects with the action of different factors. This further increases the difficulty of calculation and design. In order to meet the safety requirements of engineering projects, it is not only necessary to know the tension and slack of the towed cable, the length of the slack part, and the speed of the trawler, but also to find the specific moment and stage of the slack. These have important implications for trawl fisheries.

The trawl system can be divided into the rigid truss trawl system and fully flexible trawl system without rigid truss according to the different trawl structures. Due to its

unique flexible structure, the trawl system will inevitably deform. Its deformation leads to changes in the shape of the trawl net in both vertical and horizontal directions, namely horizontal expansion and vertical expansion, and horizontal contraction and vertical contraction, as well as overlapping between parts of the net, collision, and entanglement in three-dimensional space. The working mode of trawl system has a towing process of the trawler. In the trawl system, it is necessary to prevent uneven stress, broken nets, and excessive deformation of local nets caused by fast towing speed or fast rotation of the trawler. Due to the strong flexibility of the trawl, attention should be paid to maintaining the overall spatial shape and large expansion area of the trawl at an appropriate towing speed in order to catch more fish. At present, most of the studies are focused on the hydrodynamic performance of trawls or nets, and there are few reports on the dynamic characteristics of trawl systems during the towing process. It is necessary to study the dynamic characteristics of trawl systems during the towing process. Additionally, numerical simulation methods that consider the interaction between trawls and currents are also relatively lacking. Therefore, this paper proposed and established an equivalent mathematical model for the movement of the ocean trawl system based on the equivalent net theory. In the proposed method, the lumped mass method is used to simulate the towed cable and some lines with hydrodynamic characteristics are used to simulate the fishing net. The dynamic responses of two types of trawl systems during towing process are studied; one is the rigid truss trawl system and the other is the flexible trawl system. The effects of towing speeds on the dynamic characteristics of the truss trawl systems during straight-line towing and rotation towing are investigated using the numerical method. The rest of this paper is organized as follows. Section 2 introduces the modelling method and equivalent mathematical model for predicating the movement of the ocean trawl system. Section 3 verifies the proposed method. Section 4 discusses the dynamic response of the rigid truss and flexible trawl system during the towing process. Finally, the conclusions drawn from this paper are presented in Section 5.

2. Modelling of the Trawl System

2.1. The Lumped Mass Model

The trawl system includes the towed cable which is also known as the trawl warp. The towed cable model appears as a slender, flexible cylindrical cable. The discrete lumped mass model is used to solve the nonlinear boundary value problem. The basic idea of this model is to divide the towed cable into N segments, and the mass of each element is concentrated on one node, so that there are $N + 1$ nodes. The tension T and shear V acting at the ends of each segment can be concentrated on a node, and any external hydrodynamic load is concentrated on the node. The equation of motion of i-th node (i = 0,1 ... N) is:

$$M_{A_i}\ddot{R}_i = T_{e_i} - T_{e_{i-1}} + F_{dI_i} + V_i - V_{i-1} + w_i\Delta\bar{s}_i \tag{1}$$

Among them, R represents the node position of the cable.

$M_{Ai} = \Delta\bar{s}_i\left(m_i + \frac{\pi}{4}{D_i}^2(C_{an} - 1)\right)I - \Delta\bar{s}_i\frac{\pi}{4}{D_i}^2(C_{an} - 1)(\tau_i \otimes \tau_{i-1})$ is the mass matrix of a node; I is a 3×3 identity matrix; $T_{ei} = EA\varepsilon_i = EA\frac{\Delta s_{0i}}{\Delta s_{\varepsilon i}}$, stands for effective tension at a certain node; $\Delta s_{0i} = \frac{L_0}{(N-1)}$, represents the original length of each segment; $\Delta s_{\varepsilon i} = |R_{i+1} - R_i|$, represents the stretched length of each segment; and EA represents the axial stiffness of the cable.

F_{dI_i} represents the external hydrodynamics of each node, which is calculated according to the Morison equation [33]:

$$F_{dI_i} = \frac{1}{2}\rho D_i\sqrt{1+\varepsilon_i}\Delta\bar{s}_i(C_{dni}|v_{ni}|v_{ni} + \pi C_{dti}|v_{ti}|v_{ti}) + \frac{\pi}{4}{D_i}^2\rho C_{ani}\Delta\bar{s}_i(a_{wi} - (a_{wi}\cdot\tau_i))\tau_i \tag{2}$$

where ρ is the density of sea water, D_i is the diameter of each cable, C_{dni} is the normal drag coefficient, C_{dti} is the tangential drag coefficient, and C_{ani} is the inertia coefficient.

$V_i = \frac{EI_{i+1}\tau_i \times (\tau_i \times \tau_{i+1})}{\Delta s_{ei} \Delta s_{ei+1}} - \frac{EI_i \tau_i \times (\tau_{i-1} \times \tau_i)}{\Delta s_{ei}{}^2} + \frac{H_{i+1}\tau_i \times \tau_{i+1}}{\Delta s_{ei}}$, V represents the shear force at the node, and H represents the torsion.

The lumped mass model is shown in Figure 1. By applying a lumped-mass model, a net is assumed to be a connected structure with limited mass and spring. Lumped-mass points are set at each knot and in the center of each mesh bar. It is assumed that the mass points of knots are spherical in which the fluid force coefficients of each direction are constant, and that the mass points of the mesh bars are cylindrical elements, which means that the direction of fluid forces must be considered.

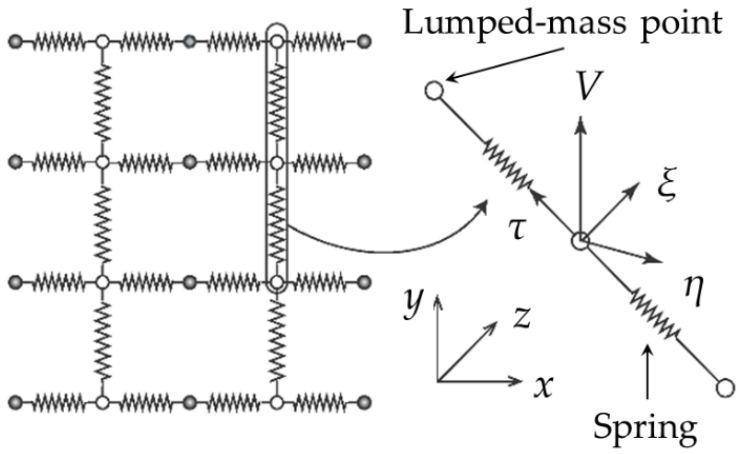

Figure 1. The lumped mass model.

2.2. Equivalent of Trawl Net

In the modeling of the trawl net, the biggest difficulty is the equivalent of the trawl net. Because of the large number of mesh, the nodes contained in the mesh can be regarded as an infinite number. The surge in the number of mesh nodes makes the model unable to converge in calculation. Therefore, it is impossible to model the actual mesh number in the modelling of the numerical model of the mesh. For the trawl net, a flexible system composed of multiple strings—in addition to using the lumped mass model proposed above for the strings that make up the net—is also necessary to perform equivalent simplification on the net to form a simplified equivalent model. The principle of equivalence is as follows:

(1) The effective area of the combined net is equal to the effective area before the combination.
(2) The diameter of the strings of the combined net is equal to the hydrodynamic force on the net before the combination.
(3) The quality of the combined net is the same as that before combination.

Figure 2 shows the equivalent model of the net. Here, k means it is the k^{th} net line and i means the node in the middle of the total horizontal distance of n adjacent net lines at the bottom edge. Assuming that the diameter of the real net line is d_0 and the hydrodynamic coefficient is C_d, the diameter of the new net line is D and the hydrodynamic coefficient is C_D; n adjacent net lines are connected into a new net line. The total volumes the net lines remain unchanged, thus leading to the following equations:

$$\frac{\pi}{4} n d_0^2 = \frac{\pi}{4} D^2 \tag{3}$$

$$D = d_0 \sqrt{n} \tag{4}$$

Assuming that the hydrodynamic coefficients before and after equivalence are equal, this leads to the conclusion that:

$$C_D = C_d \sqrt{n} \tag{5}$$

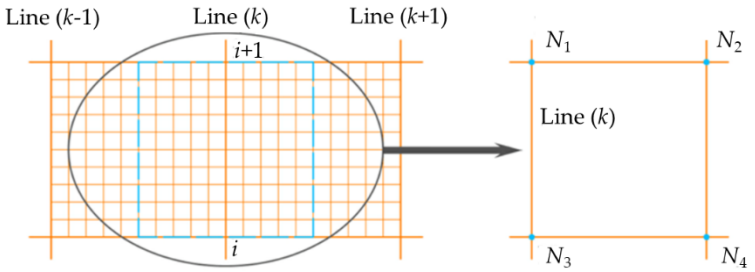

Figure 2. The equivalent model of the net.

Under the action of flow, the equivalent net model is subjected to drag loads and lift loads, as shown in Figure 3. The expressions for the horizontal drag and the vertical lift are as follows:

$$F_D = \frac{1}{2} C_D \rho A U^2 \tag{6}$$

$$F_L = \frac{1}{2} C_L \rho A U^2 \tag{7}$$

where A is the net area; ρ is the water density; U is the current velocity; and C_D and C_L are drag coefficient and lift coefficient, respectively.

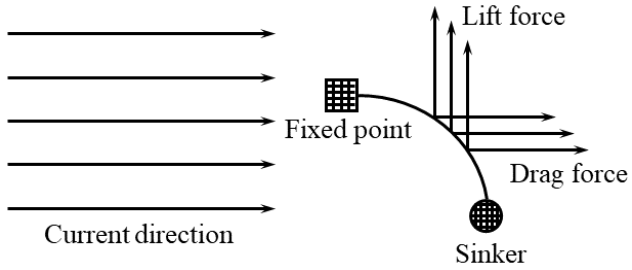

Figure 3. The load on the net.

In the study of net equivalence, the values of hydrodynamic coefficients have been widely concerned. The method of empirical formula is generally adopted. At present, Equations (8) and (9) are the most used [34].

$$C_D(S_n, \theta) = 0.04 + \left(-0.04 + 0.33S_n + 6.54S_n^2 - 4.88S_n^3\right)\cos\theta \tag{8}$$

$$C_L(S_n, \theta) = \left(-0.05S_n + 2.3S_n^2 - 1.76S_n^2\right)\sin 2\theta \tag{9}$$

where θ is the current direction angle and S_n is the water permeability of net. The relationship between drag coefficient and water permeability of net is as follows:

$$S_n = 2\frac{d_\omega}{l_\omega} - \left(\frac{d_\omega}{l_\omega}\right)^2 \tag{10}$$

The drag board and some light buoyancy balls are considered as equivalent lumped mass points. The trawl net is connected with the towed cable to form a trawl system.

2.3. Modelling of the Two Trawl Systems in OrcaFlex

In this paper, the dynamic responses of two types of trawl systems during towing process are studied; one is the rigid truss trawl system and the other is the flexible trawl system. The dynamic model is established in OrcaFlex [35]. OrcaFlex is used for the dynamic analysis of offshore marine systems, renowned for its breadth of technical capability and user friendliness. OrcaFlex also has the unique capability in its class to be used as a library, allowing a host of automation possibilities and ready integration into third party software.

For the rigid truss trawl system, due to the support of the rigid truss, the trawl can maintain a good shape and expansion area. Therefore, this kind of trawl system can be used in severe sea conditions, high-speed driving of trawlers and maneuvering conditions, and can be used to intercept and chase fish. The deformation of this kind of trawl is small in the towing process. Special attention should be paid to the tension of the towed cable and the change of the angle between the trawl and the vertical direction at different towing speeds. Excessive tension will cause the towed cable to break instantaneously. At this time, the trawl will fall and the towed cable will be suddenly lifted. Meanwhile, if the angle between the trawl and the vertical direction is too small, it is not conducive to chasing and intercepting fish. If the angle between the trawl and the vertical direction is too large, this may lead to the escape of fish.

As shown in Figure 4, the uppermost end of the rigid truss trawl is four rigid frames, which ensures that the effective fishing area of the trawl will not change. The rigid truss trawl is connected to the stern of the trawler by four towed cables. It is necessary to name the four towed cables in order to effectively analyze the fracture failure of the towed cable. When the trawler is stationary, the two cables symmetrical about the longitudinal plane of the trawler are Line Port and Line Stbd, where Line Port is on the starboard side and Line Stbd is on the port side. Both Line Lower and Line Upper are on the median plane of the trawler. Line Lower is near the stern side and Line Upper is far away from the stern.

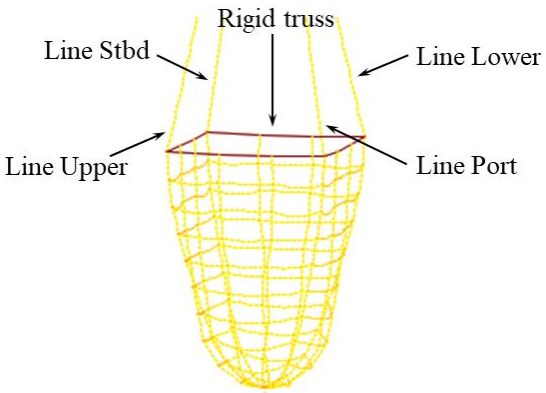

Figure 4. The rigid truss trawl.

In OrcaFlex, the material of the four rigid frame edges is a hollow homogeneous tube, and the stiffness is set to infinite. The outer diameter of the four cables is 0.35 m, the inner diameter is 0.25 m, the linear density is 0.18 T/m, the bending stiffness is 120 kN·m^2, the torsional stiffness is 80 kN·m^2, and the axial stiffness is 700,000 kN. When trawling, the Reynolds number of fishing gear is about 10^4 to 2×10^5. In order to reduce the calculation time, this paper does not consider the change of the resistance coefficient of each mass point of the fishing net with the Reynolds number, and takes the resistance coefficient and additional mass coefficient as constant values to establish the mathematical model of each mass point. The additional mass coefficient and resistance coefficient of the nodule are taken as 1.0 and 0.5, respectively. The additional mass coefficient and resistance coefficient of the foot in the x direction are taken as 0.1 and 0.0, respectively. The additional mass coefficient and resistance coefficient of the net foot in the y direction are taken as 1.2 and 1.0, respectively.

The mechanical parameters of the nets that make up the trawl are the same as those of the cables. Therefore, it can also be seen from the mechanical parameters of the nets that the trawl itself has a certain ability to resist deformation. Due to its strong anti-deformation ability, for this kind of trawl system, the overall inclination of the trawl system and the fluctuation of the towline tension are the focus of this research. Figure 5 shows the trawler and the rigid truss trawl in OrcaFlex.

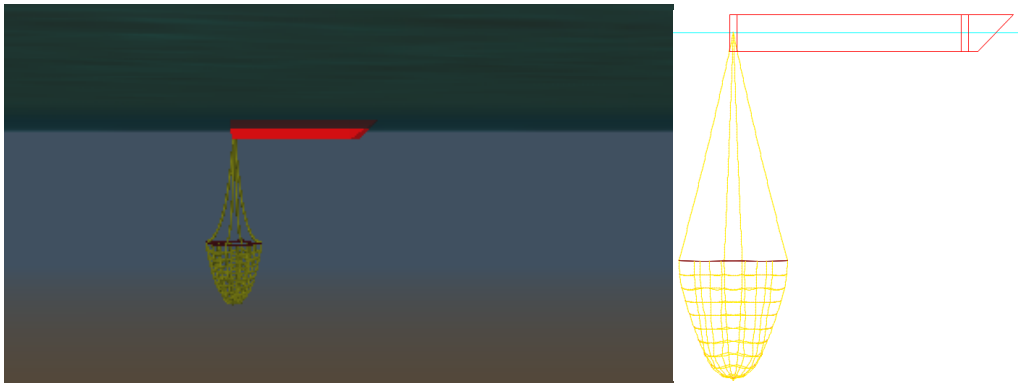

Figure 5. The rigid truss trawl system in OrcaFlex.

For the flexible trawl system, since there is no rigid frame support, it is easily deformed when pulled by the trawler, resulting in a sharp reduction in the effective fishing area. Therefore, it is not suitable for long-distance pursuit or high-speed maneuvering of trawlers to intercept fish schools. This type of trawl system is suitable for direct towing fishing in short distances and in better sea conditions. For this trawl system, the towing speed of the trawler becomes very important, and the shape of the trawling net is completely different under different towing speeds. Therefore, it is necessary to simulate the deformation of the trawl net in the single-vessel flexible trawling system under different towing speeds, to obtain the appropriate towing speed and ensure a certain effective fishing area. In the following simulation, it is assumed that the sea area where the trawl system is located is a still water sea area.

In the initial stage, the trawl net is fully deployed and fixed underwater through 8 Link components. After the simulation reaches static equilibrium, the Link is released, and the shape of the trawl net begins to change. Due to the properties of the trawl net, the nodes connected between the various net lines are represented by 3D buoys. Because the net is strongly flexible, the nodes on the real net clothing do not transmit torque and bending moments, and one of the properties of the 3D buoy is that it has translation but no rotation. Each 3D buoy only plays the role of connecting the net in this model, but the 3D buoy must have a mass to be calculated, so the mass is set to 0.1 kg, the volume is set to 0.001 m^3, and its elastic modulus is set to infinite large, regardless of the effect of the current on it. The cable and the trawl are composed of nylon cables with an outer diameter of 0.042 m, the linear density of which is 0.0016 T/m, the bending stiffness is 0, the torsional stiffness is 0, and the axial stiffness is 295 kN. Poisson's ratio is 0. From the mechanical parameters of the net, the deformation resistance of this flexible trawl is very poor (no bending resistance, very weak torsion resistance). Therefore, the deformation of the trawl net and the fluctuation of the cable tension should be studied for this trawl system. The four cables are named Line1, Line2, Line3, and Line4, respectively, according to the order of facing the bow from bottom to top, first starboard and then port. Figure 6 shows the flexible trawl system in the initial static state.

In this paper, the effects of five speeds in straight-line towing and slewing towing on the dynamic characteristics of the rigid truss trawl system are studied, which are 1, 2, 3, 4, and 5 m/s, respectively. When chasing a school of fish, in some cases, the conditions and control of the trawl position need to be carried out through the maneuvering of the trawler, in order to carry out targeted fishing. In most cases, the trawler does small radius turning maneuvers, so the turning radius of the trawler is set to be 57.32 m in the case of constant and variable radius turning. This paper also studies the effects of the turning radius on the dynamic characteristics of the rigid truss trawl system. The turning angular velocity is fixed and the turning radius is changed. In the simulation of the flexible trawl system, since the flexible trawl system rarely performs slewing operations, only the effect of speed in straight-line towing is investigated.

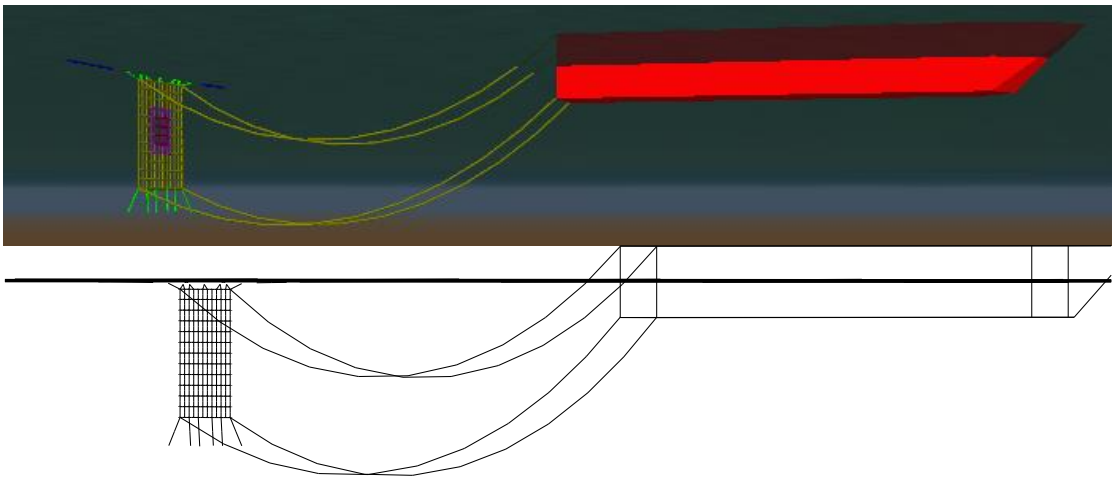

Figure 6. The flexible trawl system in OrcaFlex.

3. Validation

In order to validate the correctness of the proposed method, a numerical simulation of a trawl net was established and compared with the experiment [36]. Three types of nylon nets, types A, B, and C, were used, as shown in Table 1. Each net was set at a water depth of 1.0 m inside the flume tank. Six points on the top of each net were fixed to a steel rod (1.5 m long) on the water surface and the two bottom corners were fixed to two sinkers under the flow (Figure 5). The current velocity was set at 16.1, 19.5, 23.7, 28.0, 32.4, 36.9, and 40.9 cm/s. Figure 7 shows the diagram of the validation model.

Table 1. The net types.

Net Type	Twine Diameter/mm	Mesh Size/mm	Total Mass/g
A	0.348	75	9.91
B	0.348	50	14.68
C	0.348	40	22.31

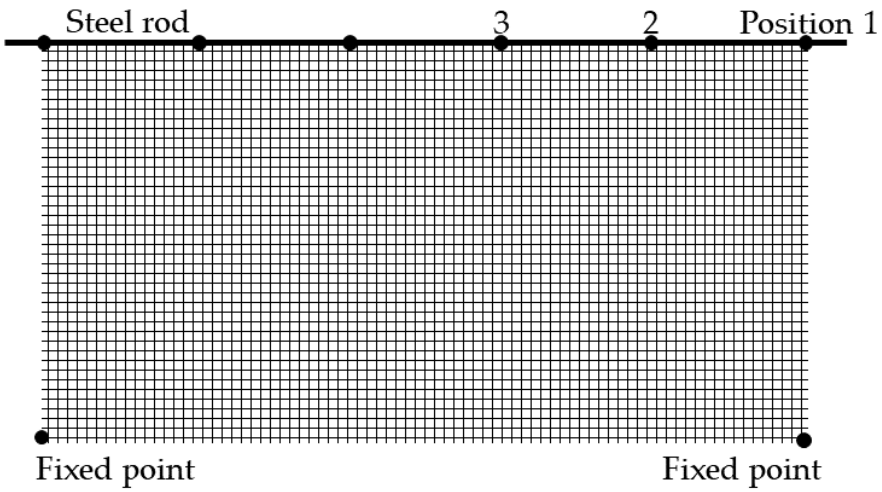

Figure 7. The diagram of the validation model.

Figure 8 shows the comparison of the flow component for loads acting on the steel rod between the simulation and experiment. Figures 9–11 show the comparison of tension loads at three positions of different net types. Overall, the numerical simulation method is in good agreement with the experimental results. For the flow loads acting on the steel rod, the numerical results fit well with the experimental results, and the errors are within 5%.

Compared with the experiment, some numerical results of tension load at three positions are not consistent, such as 23.7 cm/s at position 1 of type A, and 16.1 cm/s and 32.4 cm/s at position 1 of type B. The reason is that the tension of the mesh along the diagonal direction of the rectangular mesh in the simulation is larger than that in the flume test. The general trend of simulation is consistent with that of experiments. The numerical method is able to estimate the loads on the net. It should be noted that the calculation requires a considerable investment of time, because the fishing net is modeled as a large number of mass points, equal to the number of knots and mesh bars. Therefore, it is necessary that calculation models with grouped mass points are used appropriately, by taking the desired accuracy of the estimation into account.

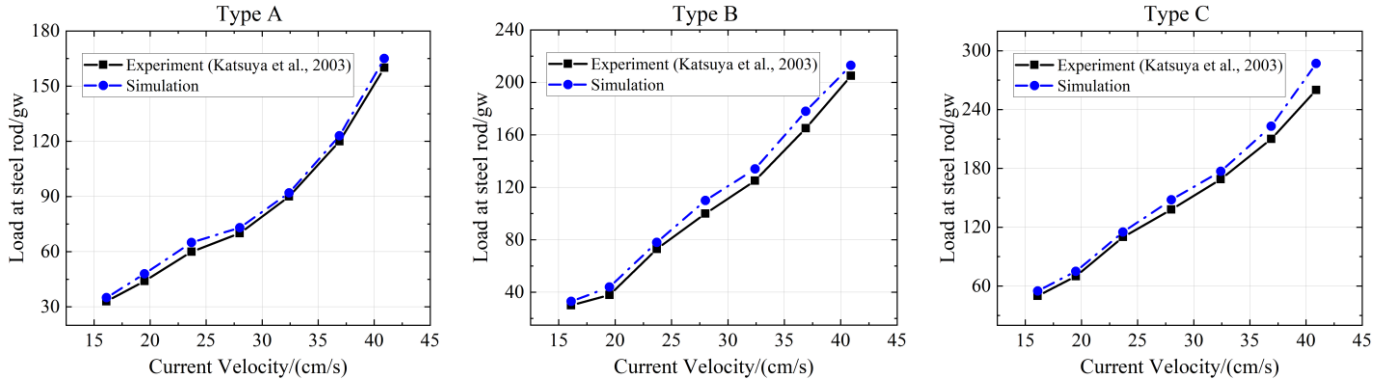

Figure 8. The comparison of the flow component for loads acting on the steel rod [36].

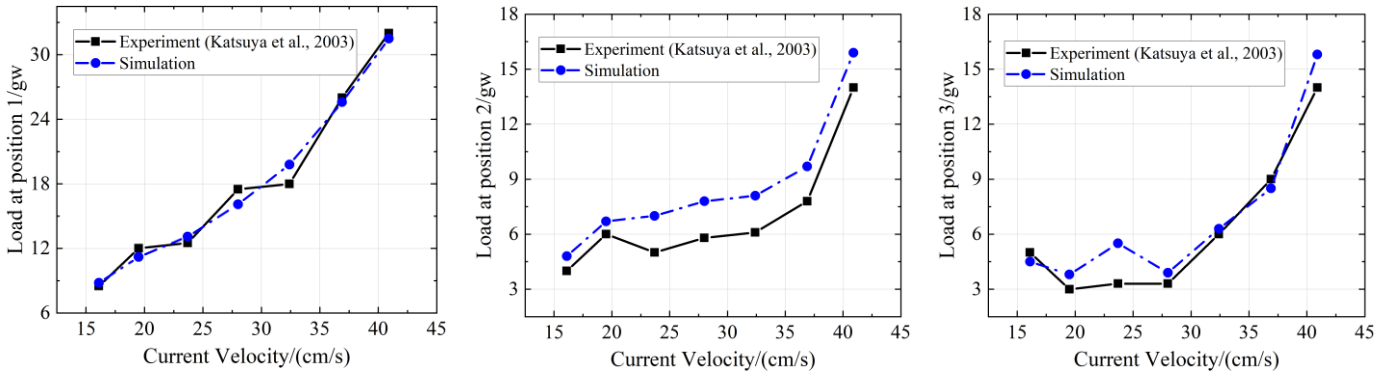

Figure 9. The comparison of the tension loads of net type A [36].

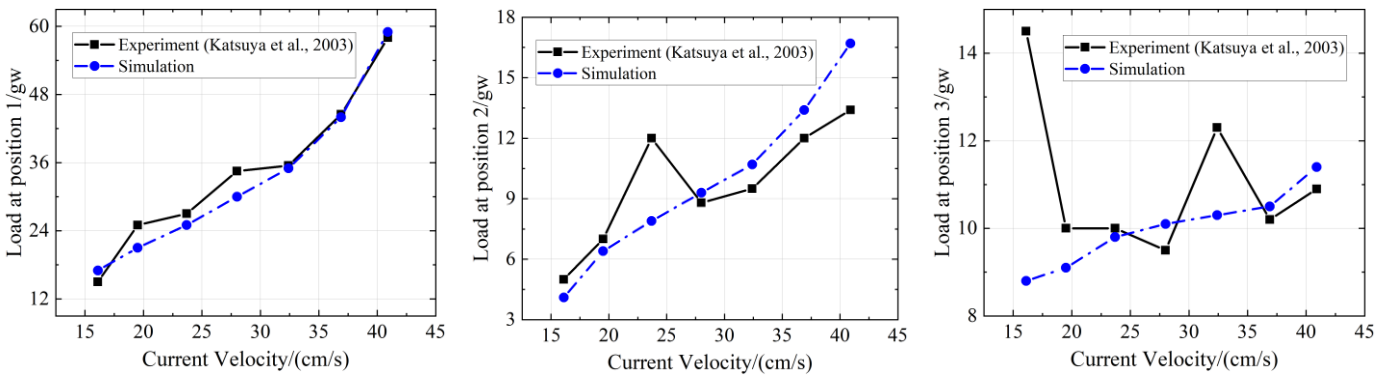

Figure 10. The comparison of the tension loads of net type B [36].

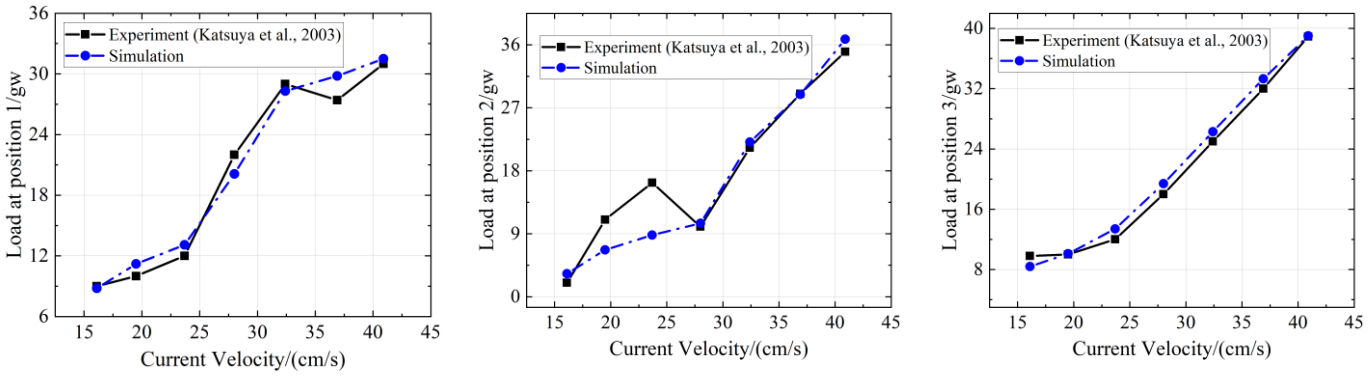

Figure 11. The comparison of the tension loads of net type C [36].

4. Results and Discussion

4.1. Dynamic Response of the Rigid Truss Trawl System

Figure 12 shows the tension of the four cables in time domain under different speeds. It can be seen from Figure 12 that, when the towing speed of the trawler is low, the tension of the cable hardly changes in the whole time domain. When the towing speed is high, the tension of the cable increases from low to high. After the tension is stable, the tension of the four cables increases with the increase of the towing speed. With the increase of towing speed, the moment when the tension of the cable begins to increase sharply in the time domain keeps moving forward, and the change rate of the tension also increases with the increase of the towing speed. In this state, the cable is mainly subjected to the tension. Although it is slightly bent, the tension makes the cable straighten in the axial direction. Therefore, the bending deformation of the cable is very weak in straight-line towing. Although the bending deformation of the cable is almost negligible, due to the bending stiffness of the cable itself, the existence of this stiffness and the tension of the cable keeps the trawl from deforming during the towing process. Therefore, although the bending deformation is very weak, the cable is still affected by the bending moment. The maximum bending moment occurs near 1.5 m at the end of the connection between each cable and the tail end of the trawler.

Figures 13–17 show the shape changes of the trawl at different towing speeds. During the straight-line towing process, the rigid truss trawl itself does not have large deformation, and the change of the inclination of the rigid truss trawl mainly focuses on the change of the angle between the trawl and the vertical direction. With the increase of the towing speed, the angle between the rigid truss trawl and the vertical direction gradually increases after reaching stability, and the longitudinal offset of the trawl away from the stern direction is greater. On the one hand, the effective fishing area of the trawl increases with the increase of the towing speed, and the inclination angle between the trawl and the vertical direction, which is conducive to the entry of the fish into the net when chasing the fish. On the other hand, as the towing speed increases, the depth of the whole trawl in the water gradually decreases after stabilization. The increase of the angle between the trawl and the vertical direction means that the angle between the trawl and the horizontal direction decreases. When the speed reaches a certain degree, the whole trawl is parallel to the horizontal direction. In this case, the fish are more likely to escape from the net. Furthermore, the spatial attitude change of the trawl is mainly concentrated in the two-dimensional plane *x*-*z*. The trawl mainly occurs in the uniform translational motion in the *x* direction, a small increase in the z direction, and the angle changes between the trawl and the vertical Z axis. Therefore, when the trawler is sailing at a high speed, it is helpful to chase the fish and make the fish enter the net quickly. However, at the moment when the fish enter the net, it is necessary to quickly shorten the length of the cable to increase the inclination angle between the trawl and the horizontal direction, so as to avoid the fish that have been captured escaping again.

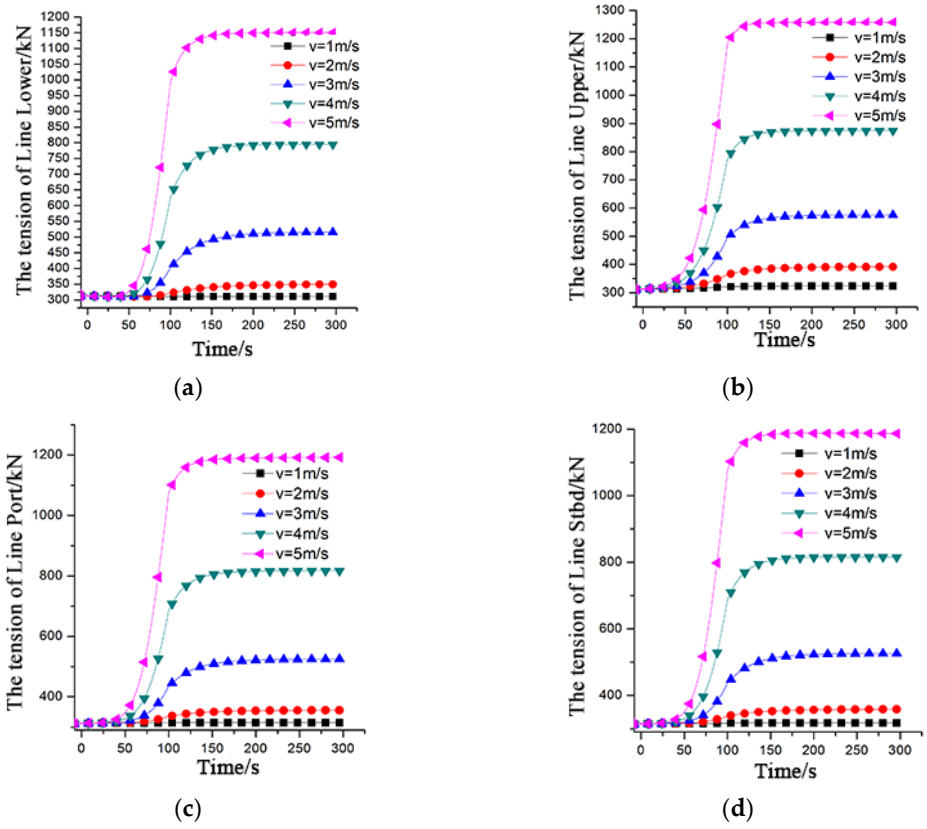

Figure 12. The time domain image of cables tension of the rigid truss trawl system in straight-line towing: (**a**) Line Lower; (**b**) Line Upper; (**c**) Line Port; (**d**) Line Stbd.

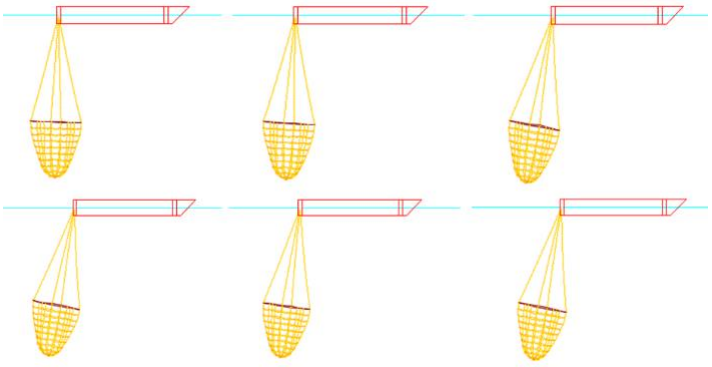

Figure 13. Shape changes of rigid truss trawl in straight-line towing at v = 1 m/s.

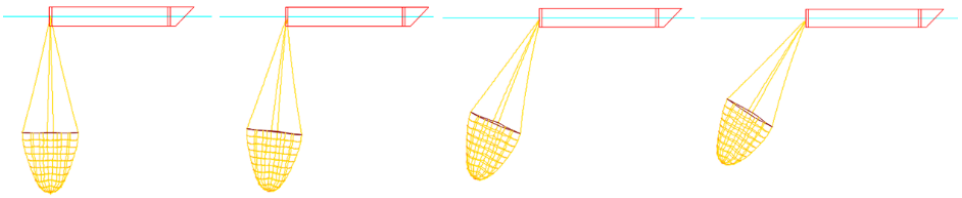

Figure 14. Shape changes of rigid truss trawl in straight-line towing at v = 2 m/s.

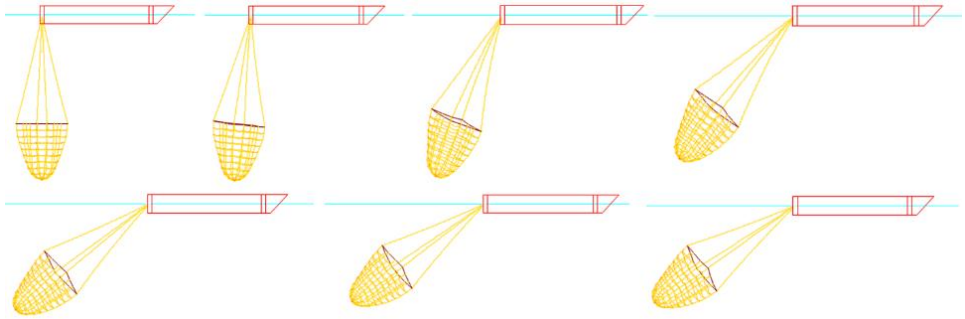

Figure 15. Shape changes of rigid truss trawl in straight-line towing at v = 3 m/s.

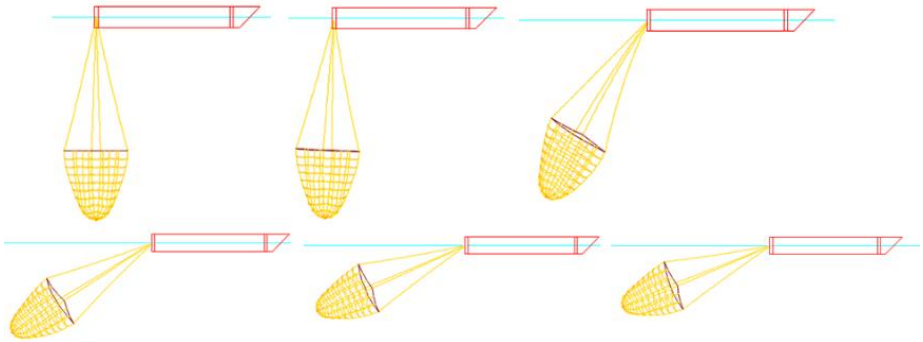

Figure 16. Shape changes of rigid truss trawl in straight-line towing at v = 4 m/s.

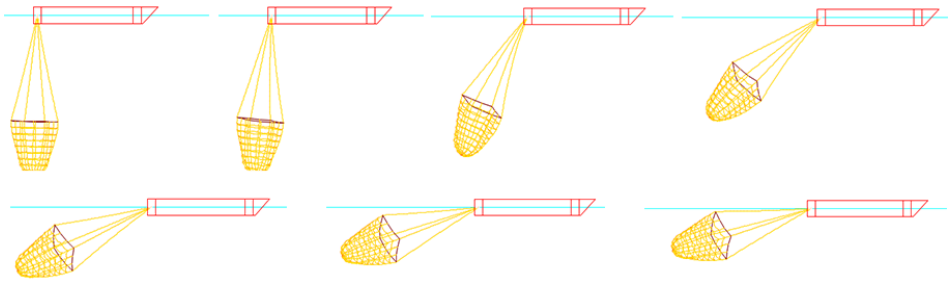

Figure 17. Shape changes of rigid truss trawl in straight-line towing at v = 5 m/s.

In most cases, the trawler does small radius turning maneuvers, so the turning radius of the trawler is set to be 57.32 m. Figure 18 shows the time domain image of cable tension of the truss trawl system in rotating towing under a fixed turning radius. In this section, the range of angular velocity is 1–5°/s, which is determined by the general expression of centripetal acceleration $a = \omega^2 R$. During the turning process, in order to make the trawl turn with the trawler, the component in the tension of the towed cable should provide the centripetal force to make the trawl turn. Assuming that the mass of the whole trawl system at a certain time is m, the expression of this part of the tension component is $F = m\omega^2 R$. That is to say, with the increase of the angular velocity, the component of the cable tension which maintains the turning of the trawl will increase sharply with respect to the square of the angular velocity, rather than a linear increase with respect to the angular velocity. Therefore, when the angular velocity continues to increase to a certain extent, ω^2 will become very large, so the tension of the cable will also become very large. Excessive tension will eventually lead to the strong destruction of the boundary conditions that maintain the rigid frame edges. In this case, the trawl will fall apart completely. In order to test this hypothesis, this paper calculates the limit angular velocity of the rigid trawl on the premise of keeping the turning speed at 1 m/s. After continuous debugging and calculation, it is found that when the angular velocity is 20°/s, the square frame composed of four rigid frame edges can still remain closed and the shape is basically unchanged, so the shape of the

trawl can still remain basically stable. As the return angular velocity continues to increase, the square frame begins to deform significantly and the deformation will gradually increase. When the angular velocity increases to a certain extent, the deformation of the frame edge reaches the limit that can be restrained, and the square frame is completely unstable. It is found that when the angular velocity is 57.3°/s, the trawl will be completely scattered. The specific situation is shown in Figure 19.

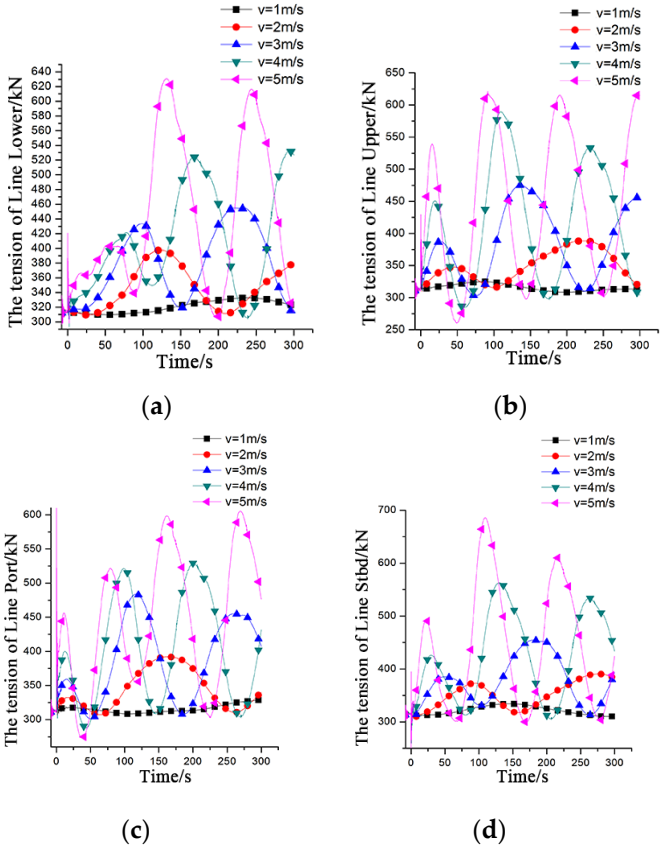

Figure 18. The time domain image of cables tension of the rigid truss trawl system in rotating towing under fixed turning radius: (**a**) Line Lower; (**b**) Line Upper; (**c**) Line Port; (**d**) Line Stbd.

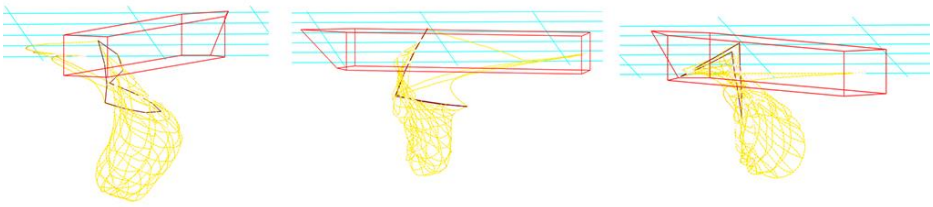

Figure 19. Shape changes at large angular velocity.

Figures 20–24 show the shape changes of the rigid truss trawl in rotating towing under fixed turning radius at different speeds. When the trawler is turning, the angle between the rigid truss trawl and the vertical direction changes. A remarkable feature is that it will rotate around its own central axis and drift out in the opposite direction to the instantaneous rotation direction. This outward drift is sometimes inclined to the port side of the trawler and sometimes to the starboard side of the trawler. It will also move away from or close to the stern. At any time in the process of turning, the outward drift of the trawl is a composite motion of these motions. When the torsion is too large, the outward drift will cause the four cables to entangle with each other near the top connected to the trawler, which will also increase the tension on the streamer. When the trawler returns, the streamer will not only be subject to tension and bending, but also be subject to torsion.

The spatial attitude of the trawl will also change to become more complex in the rotating state. The spatial attitude change of the trawl mainly focuses on the change of the angle between the trawl and the vertical direction when the trawler is sailing directly. The spatial attitude change of the trawl can be reflected in the two-dimensional x-z plane of the overall coordinate system. During the turning of the trawler, on the one hand, the outward drift of the trawl will occur in the three-dimensional coordinate system; on the other hand, its torsion around its own central axis also needs to be observed in the vertical direction. Therefore, the change of trawl attitude under the turning state of the trawler will be in the three-dimensional space. After rough observation, it is found that the trawl has two degrees of freedom of translation and one degree of freedom of rotation when the trawler is sailing directly, while the trawl has three degrees of freedom of translation and two degrees of freedom of rotation when the trawler is turning.

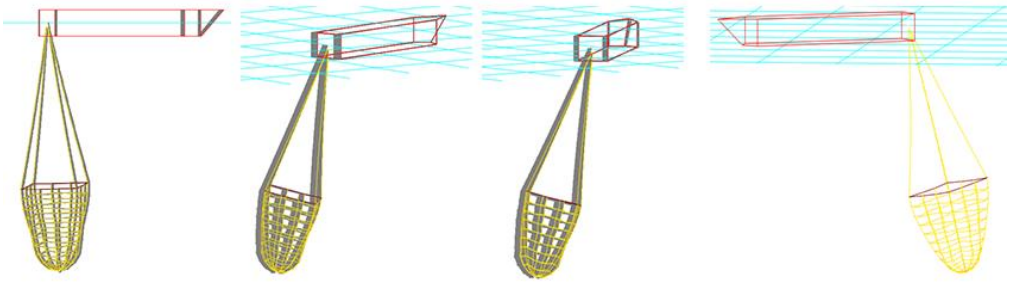

Figure 20. Shape changes of rigid truss trawl rotating towing under fixed turning radius at v = 1 m/s.

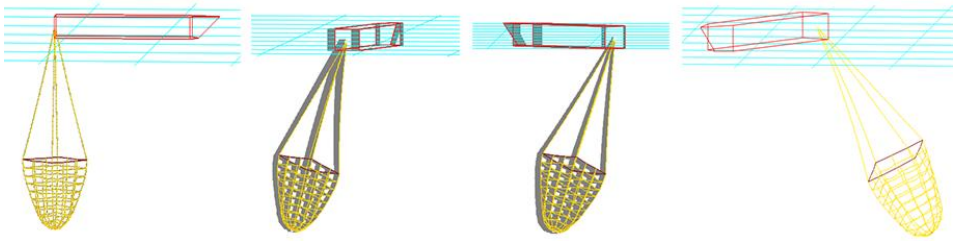

Figure 21. Shape changes of rigid truss trawl rotating towing under fixed turning radius at v = 2 m/s.

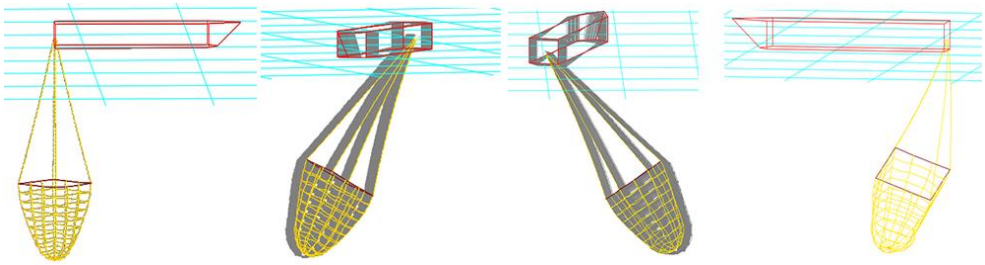

Figure 22. Shape changes of rigid truss trawl rotating towing under fixed turning radius at v = 3 m/s.

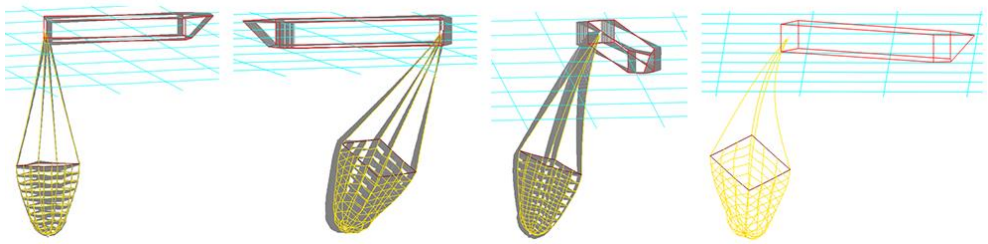

Figure 23. Shape changes of rigid truss trawl rotating towing under fixed turning radius at v = 4 m/s.

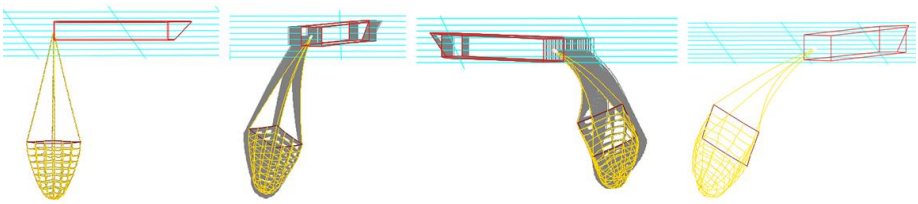

Figure 24. Shape changes of rigid truss trawl rotating towing under fixed turning radius at v = 5 m/s.

Further observation shows that with the increase of towing speed, the overall outward floating distance of the trawl increases gradually under the condition of fixed turning radius. With the increase of the outward floating distance, the tension of the four cables will increase in varying degrees. The tensions of the cables in the turning state have a sudden change in the initial stage, and then show a periodic fluctuation in the time-domain, while the tensions will eventually reach a stable value during the straight-line towing.

In fact, under the premise of fixed turning radius, with the increase of angular velocity, the change rate of the turning angle in the horizontal plane also increases, which leads to the increase of the outward floating distance of the trawl currently. When the trawler is turning at different angular speeds, the increase of the angular speed will lead to the increase of the floating distance of the trawl and the tension of the cable. Because of the periodical change of the turning, the floating distance of the trawl and the tension of the cable also change periodically in the time domain. With the increase of the angular velocity of the trawler, the period of this fluctuation becomes shorter.

The effects of the speeds under fixed angular velocity are also studied. The angular velocity of the trawler is constant at 1°/s. In essence, it explores the effects of turning radius on the dynamic characteristics of the rigid truss trawl.

Figure 25 shows the time domain image of the tension of the four cables in rotating towing under fixed angular velocity. It can be found that among all the factors affecting the increase of cable tension, the towing speed plays a decisive role. Therefore, on the premise that the floating distance of the trawl decreases, the cable tension will continue to increase with the increase of towing speed. In this case, the angular velocity is very small, so the fluctuation periodicity of the tension in the time domain under different towing speeds becomes not obvious, and tends to be stable with the increase of the towing speed, which indicates that at low angular velocity, with the increase of the turning radius, it is easier for the cable tension to achieve stability. In this case, the change of tension in the time domain is less severe than that in the time domain when the radius of gyration is fixed. This phenomenon is caused by the expression a of centripetal acceleration $a = \omega^2 R$. It can be seen that the component of the tension overcoming the centripetal force is directly proportional to the square of the angular velocity when the turning radius is fixed, while the component of the tension providing the centripetal force and the turning radius show an obvious linear relationship when the turning angular velocity is fixed. It is the difference in the change law of this tension component in the two states that leads to the complete difference in the fluctuation of the cable tension in the two cases.

It can be seen from the calculation results under the two turning states that the four cables will also have obvious bending deformation in rotating towing, which is completely different from the very weak bending deformation of the cables during straight-line towing. During the turning process, the increase of the towing speed, the increase of the floating distance of the trawl, and the increase of the angular velocity will lead to the increase of the cable tension. Among the above factors, the increase of angular velocity has the most obvious effect on the floating distance and deformation of the trawl. However, under the action of rigid frame edge, when the cable is normal, the width of the mesh port remains unchanged, but the height of the mesh port is different in different towing operations.

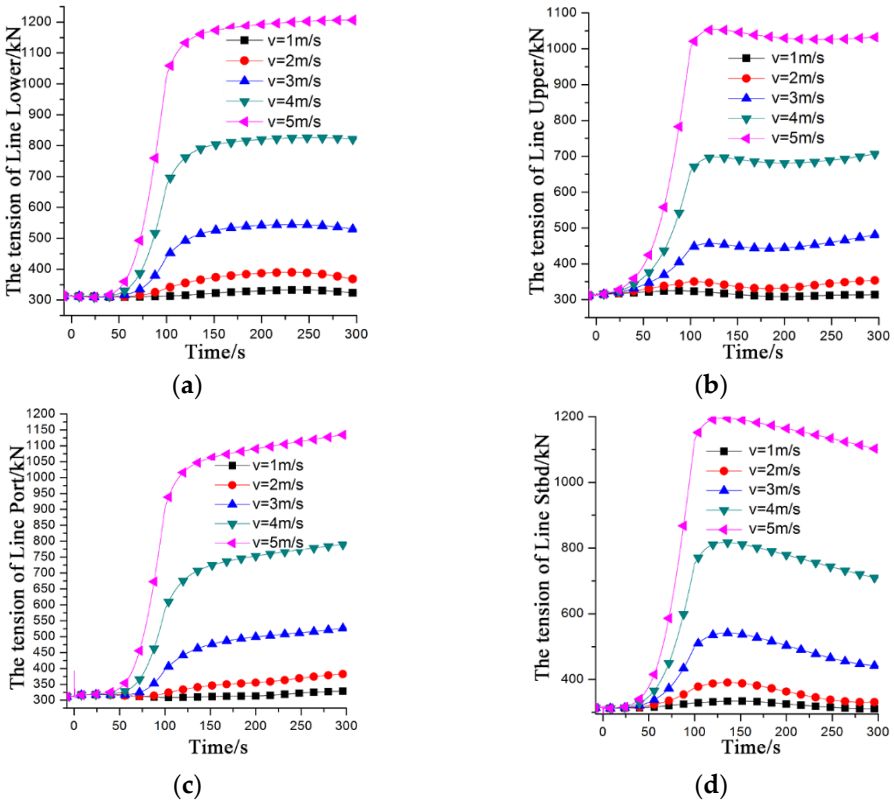

Figure 25. The time domain image of the cables' tension of the rigid truss trawl system in rotating towing under fixed angular velocity: (**a**) Line Lower; (**b**) Line Upper; (**c**) Line Port; (**d**) Line Stbd.

Figures 26–30 show the shape changes of the trawl in rotating towing under fixed angular velocity at different speeds. When the angular velocity is constant, the increase of towing speed mainly depends on the increase of turning radius. In this case, as the towing speed increases, the turning radius should also increase. However, with the increase of turning radius, the floating distance of the trawl will decrease at the same time. The reason for this phenomenon is analyzed as follows: although the essence of the increasing speed in this case is caused by the increase of the turning radius for maneuvering steering, with the increase of the turning radius, the unit horizontal displacement of the trawler causes the deflection angle of the trawler in the horizontal plane to change. On the contrary, the rate of change gradually decreases, which indirectly leads to the decrease of the drifting distance of the trawler.

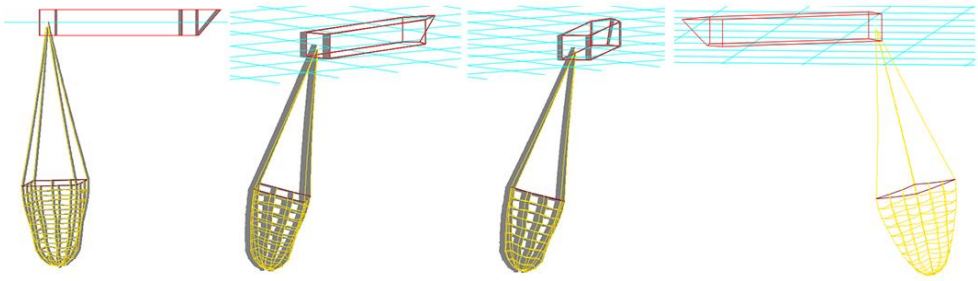

Figure 26. Shape changes of rigid truss trawl in rotating towing under fixed angular velocity at $v = 1$ m/s.

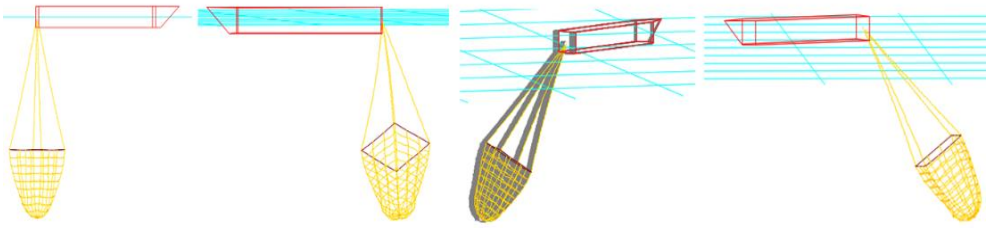

Figure 27. Shape changes of rigid truss trawl in rotating towing under fixed angular velocity at $v = 2$ m/s.

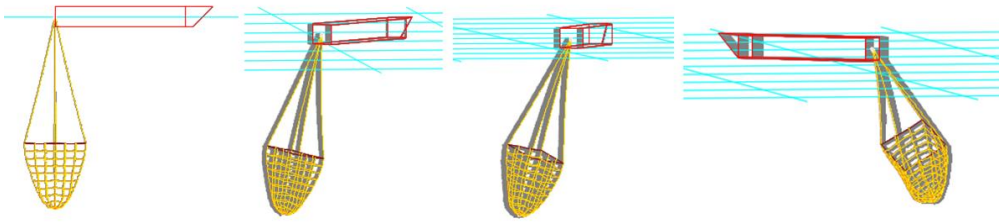

Figure 28. Shape changes of rigid truss trawl in rotating towing under fixed angular velocity at $v = 3$ m/s.

Figure 29. Shape changes of rigid truss trawl in rotating towing under fixed angular velocity at $v = 4$ m/s.

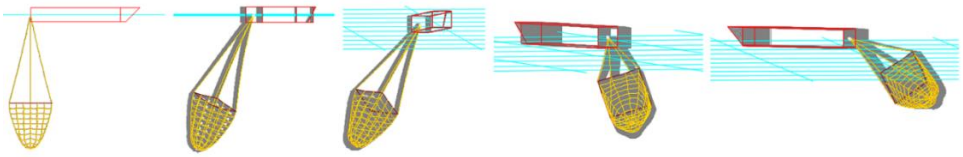

Figure 30. Shape changes of rigid truss trawl in rotating towing under fixed angular velocity at $v = 5$ m/s.

4.2. Dynamic Response of the Flexible Trawl System

Figure 31 depicts the tension of the cables of the flexible trawl system in straight-line towing. For a single cable, as the towing speed of the trawler increases, its cable tension increases continuously. At a certain trawler towing speed, with the increase of time, the growth trend of cable tension slows down; moreover, with the increase of trawler towing speed, the cable tension increases simultaneously. Observing the fluctuations of the four cables in the time domain, respectively, the expansion and contraction changes of the four streamers in the entire trawl system have good synchronization and coordination, and the tension of the four streamers at the same towing speed fluctuates in the time domain The curves are not much different. Further observation shows that when the drag speed of the trawler is low, the drag tension of the drag chain reaches a stable level in a short time (1 m/s in this simulation). The time required for the traction tension to stabilize is greatly increased. When the towing speed of the trawler is greater than or equal to 3 m/s, the cable tension has been increasing within the time range set in this simulation, and has not yet reached stability.

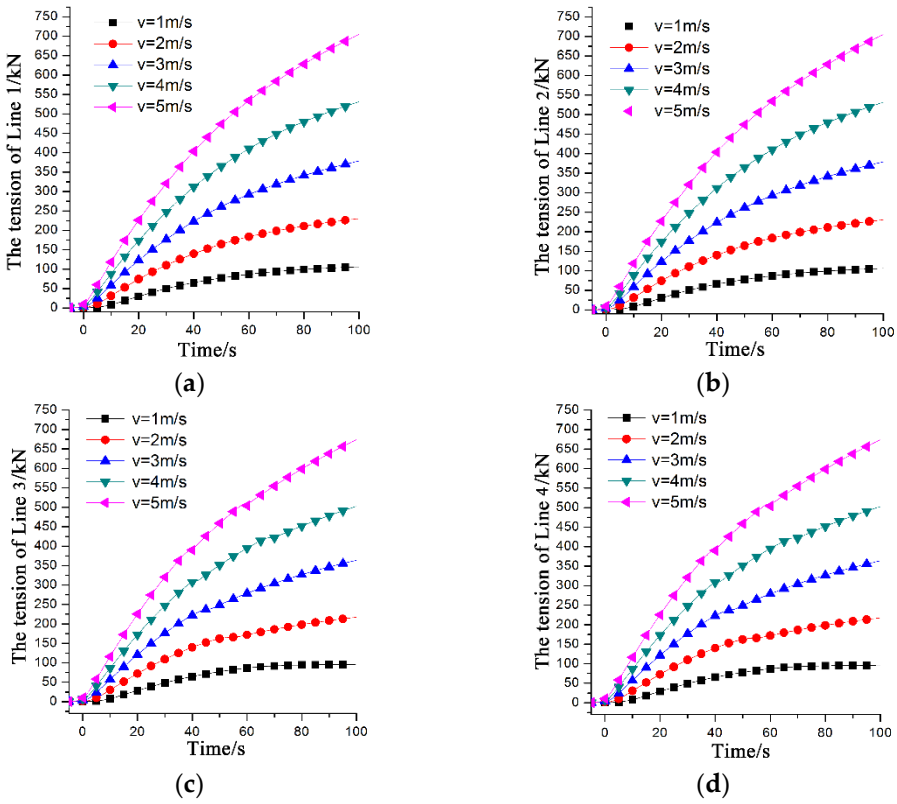

Figure 31. The time domain image of the cables' tension of the flexible trawl system in straight-line towing: (**a**) Line1; (**b**) Line 2; (**c**) Line 3; (**d**) Line 4.

Figures 32–36 show the shape changes of the flexible trawl in straight-line towing at different speeds. During the entire towing process, the flexible trawl first sinks under its own gravity after it is fully opened until fully submerged in water. As the trawler moves forward, the flexible trawler is pulled vertically by the cable. The effective fishing area begins to shrink, and the opening width of the trawl net becomes smaller. The uppermost part of the flexible trawl near the two cables has been pulled above sea level under the constant pulling action of the trawler. Further observation shows that there is a trawling shape that can make the trawling completely horizontal and has the largest effective fishing area under different towing speeds of the trawler. After this state, the trawl net begins to pitch and tilt while the effective fishing area continues to shrink under the action of the cable. With the continuous reduction of the effective fishing area of the trawl, the pitch and tilt of the trawl will gradually disappear. Since the flexible trawl has no bending resistance at all, when the length of the cable is long and the trawler sails a large distance, the trawl is finally compressed into upper and lower layers. Finally, the two layers will be folded repeatedly around a line of mesh at the intersection of the upper and lower layers, making the effective fishing area extremely small. The effect of different towing speeds on the shape changes of the flexible trawl is mainly reflected in the difference in the time when the flexible trawl reaches a certain shape and the tension of the cable. It is found in the simulation that the faster the towing speed of the trawler, the less time it takes for the flexible trawl to reach a certain shape, and the shorter the sailing distance of the trawler. The slower the towing speed of the trawler, the longer it takes for the flexible trawl to reach a certain shape, and the longer the trawler travels. If the drag distance is large enough, the final configuration of the flexible trawl should be the same at low and high speeds. This also verifies the conclusion that this pure flexible trawl system is more suitable for fishing in short distances. Therefore, for this flexible trawl system, it is necessary to find out the most suitable range of trawler sailing distance under different towing speeds, and select the appropriate towing speed of the trawler according to the path of the actual fish

school, the distance between the fish school and the local sea conditions, to achieve the best fishing results.

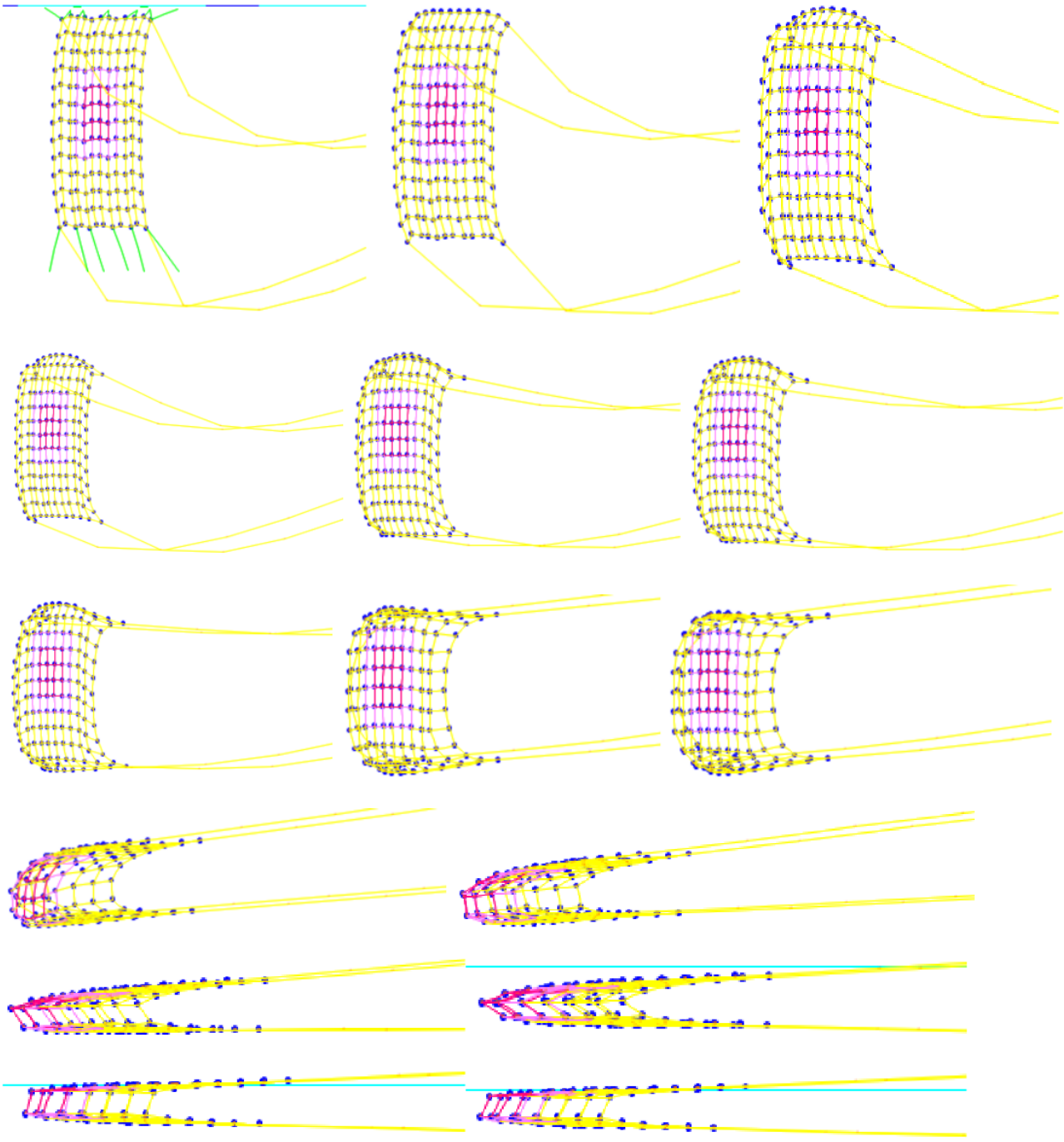

Figure 32. Shape changes of the flexible trawl in straight-line towing at v = 1 m/s.

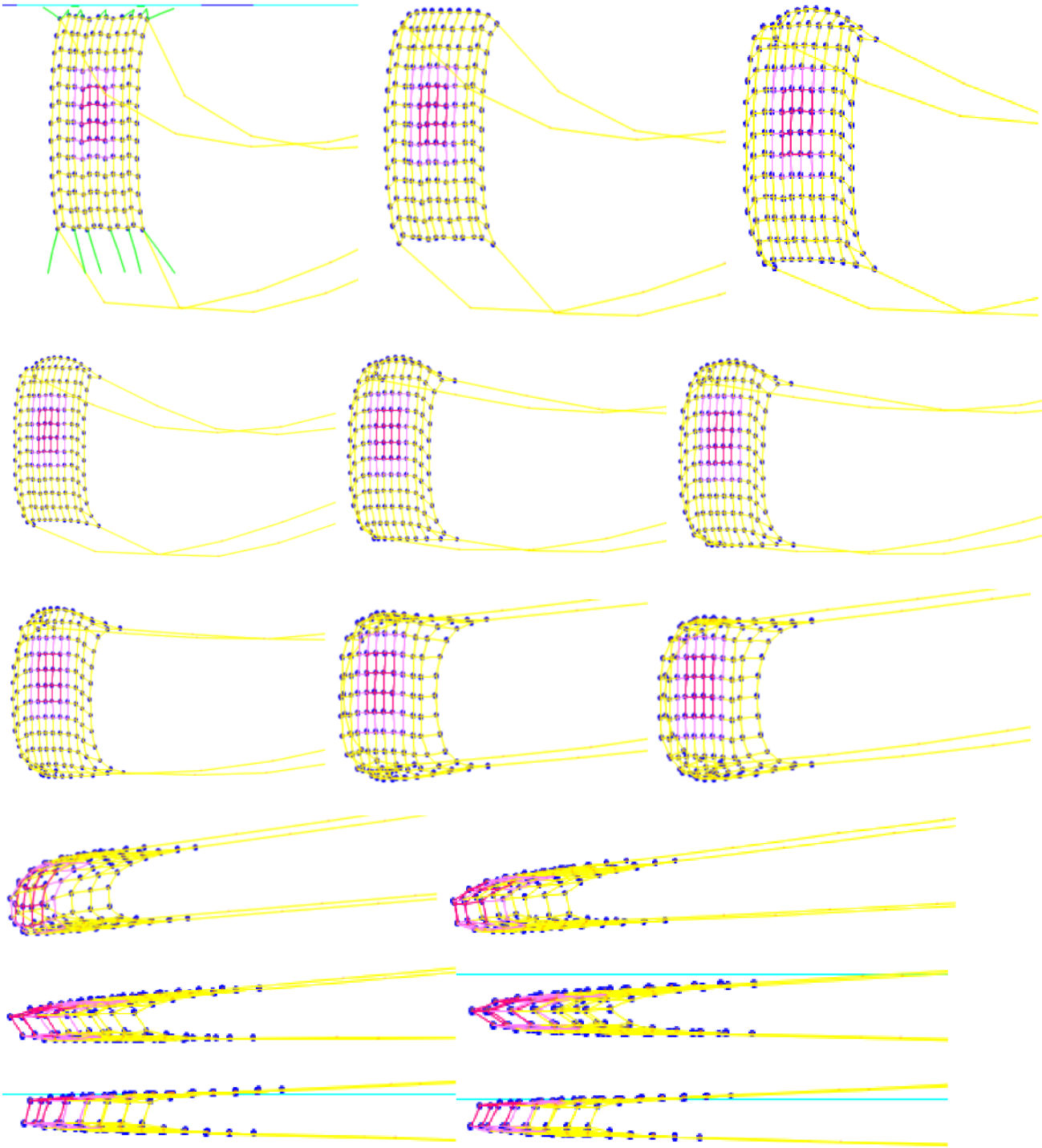

Figure 33. Shape changes of the flexible trawl in straight-line towing at v = 2 m/s.

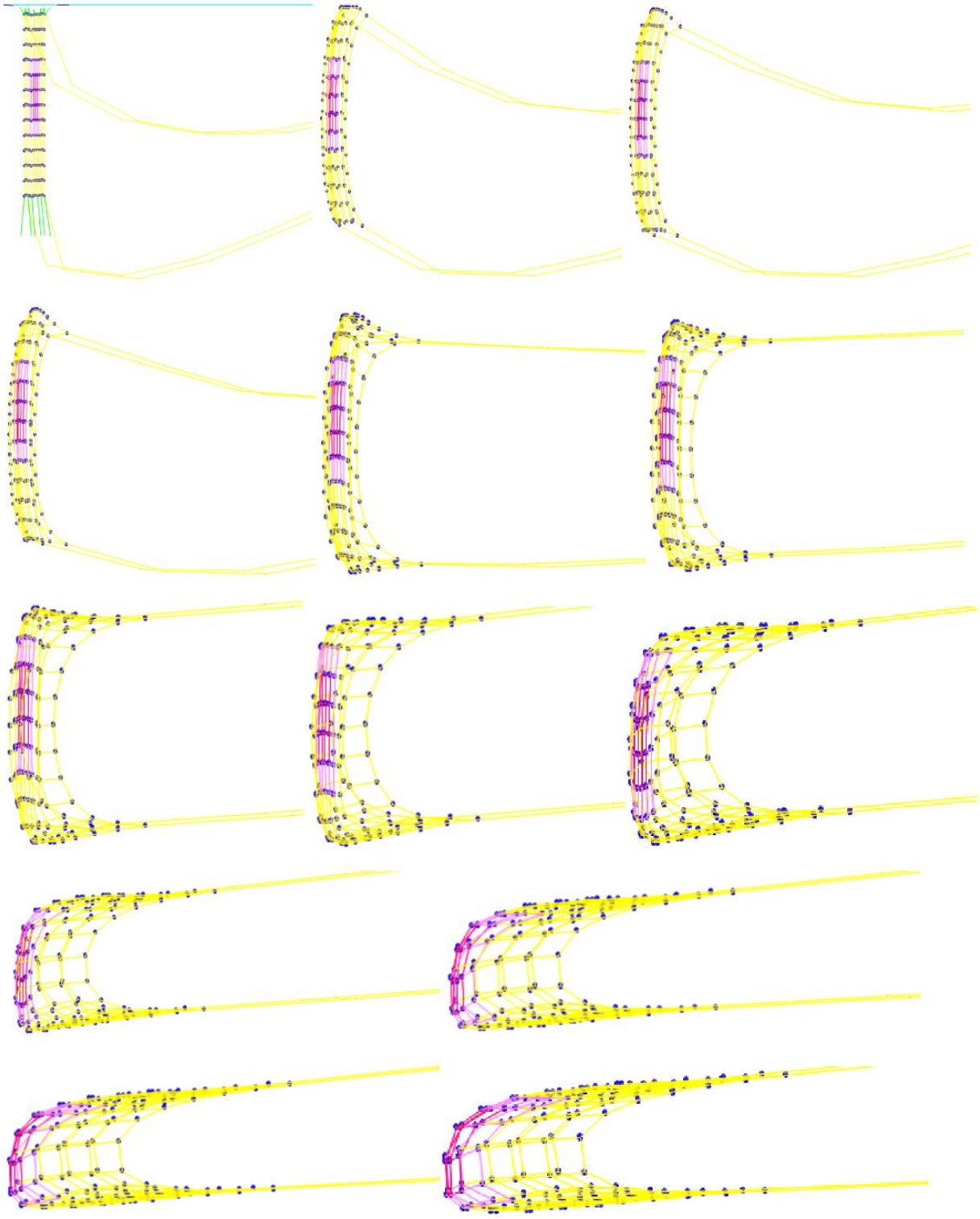

Figure 34. *Cont.*

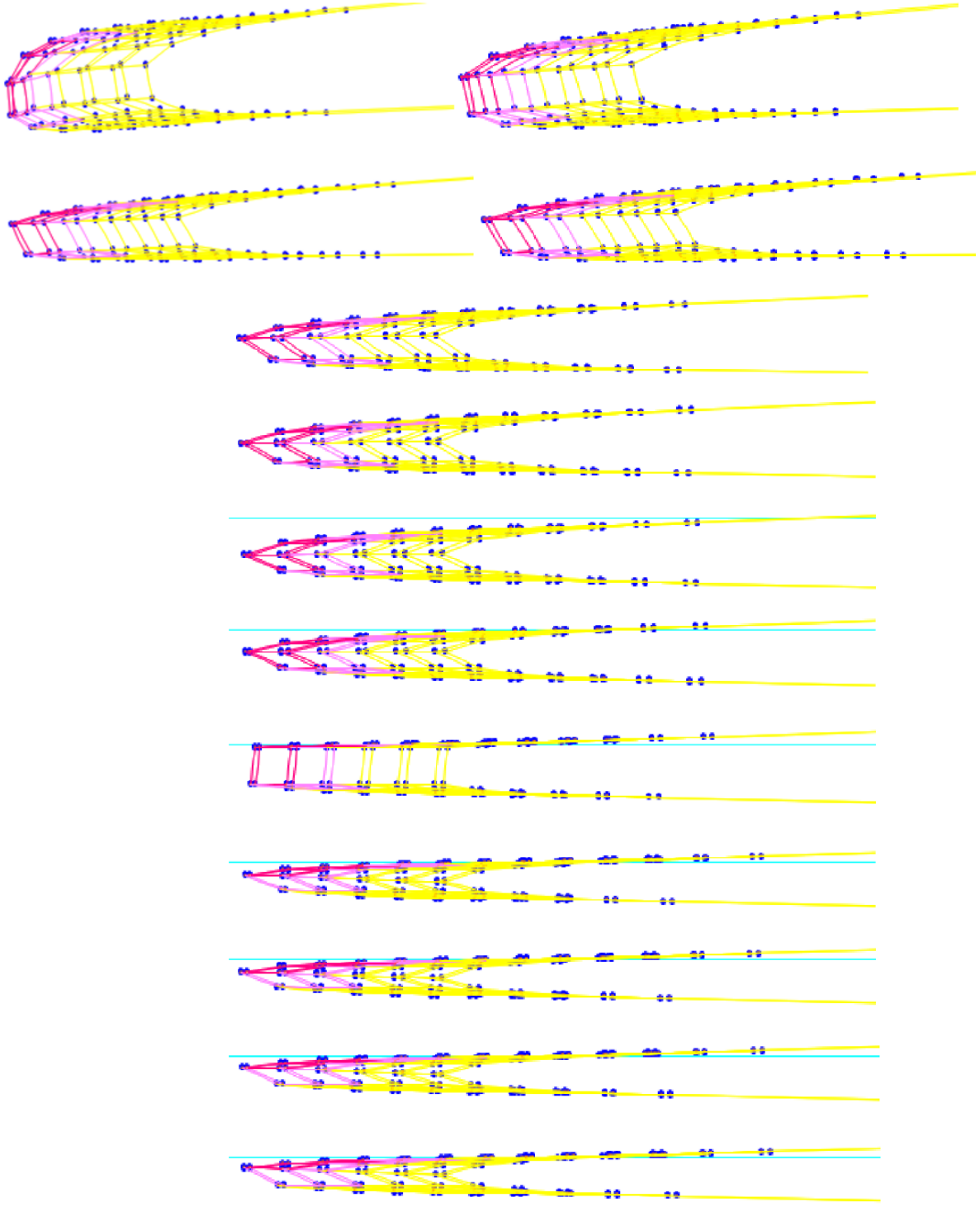

Figure 34. Shape changes of the flexible trawl in straight-line towing at v = 3 m/s.

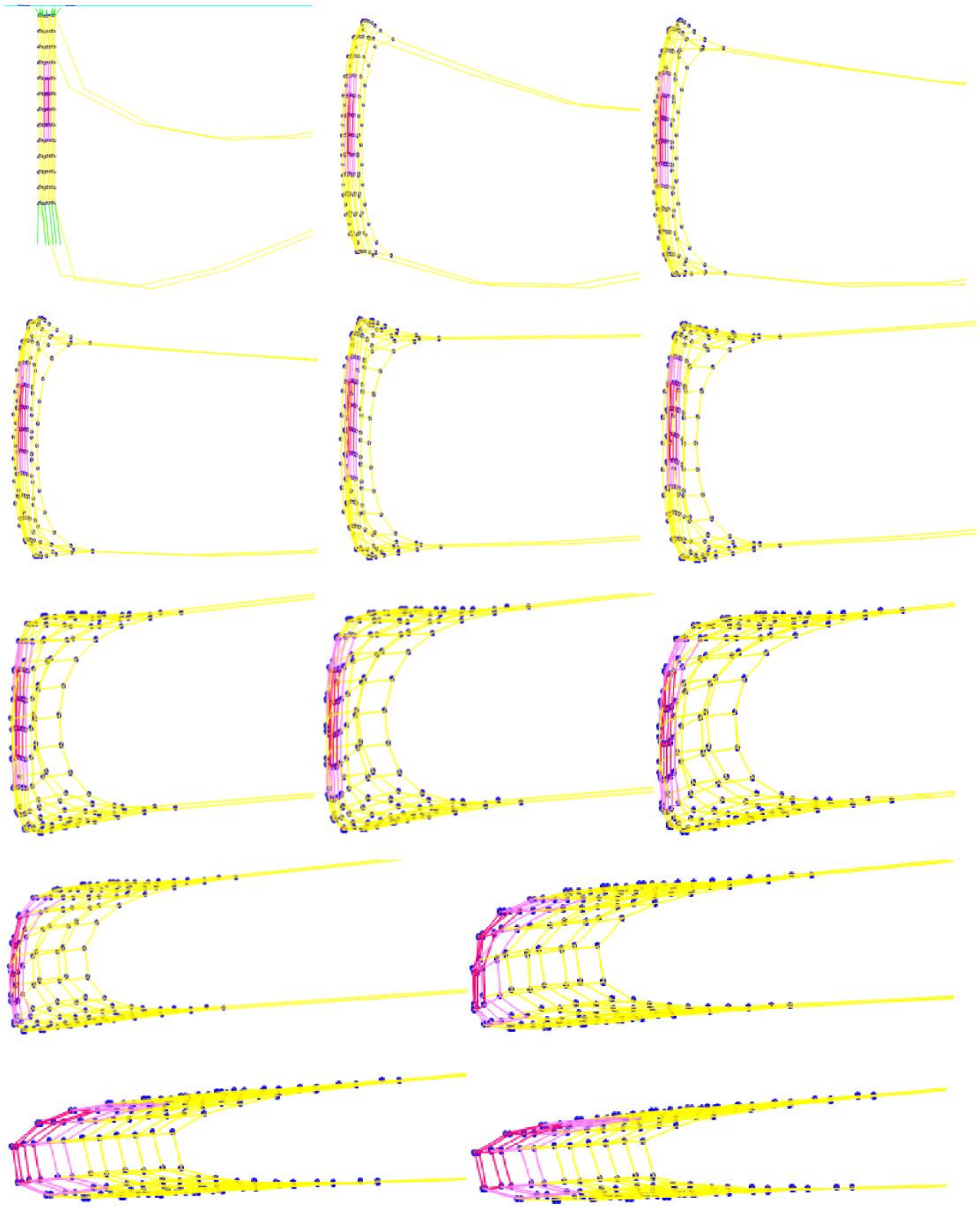

Figure 35. *Cont.*

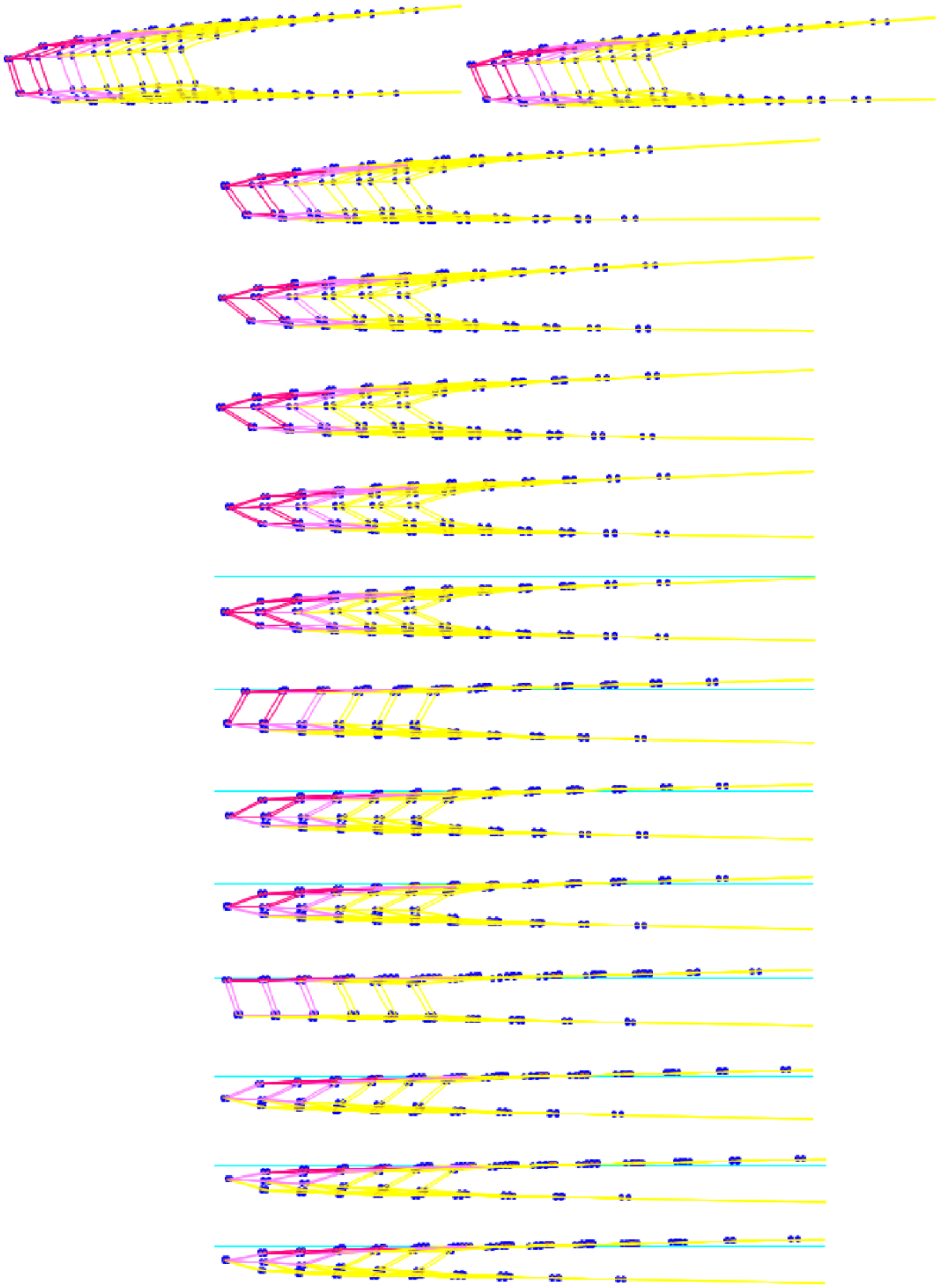

Figure 35. Shape changes of the flexible trawl in straight-line towing at v = 4 m/s.

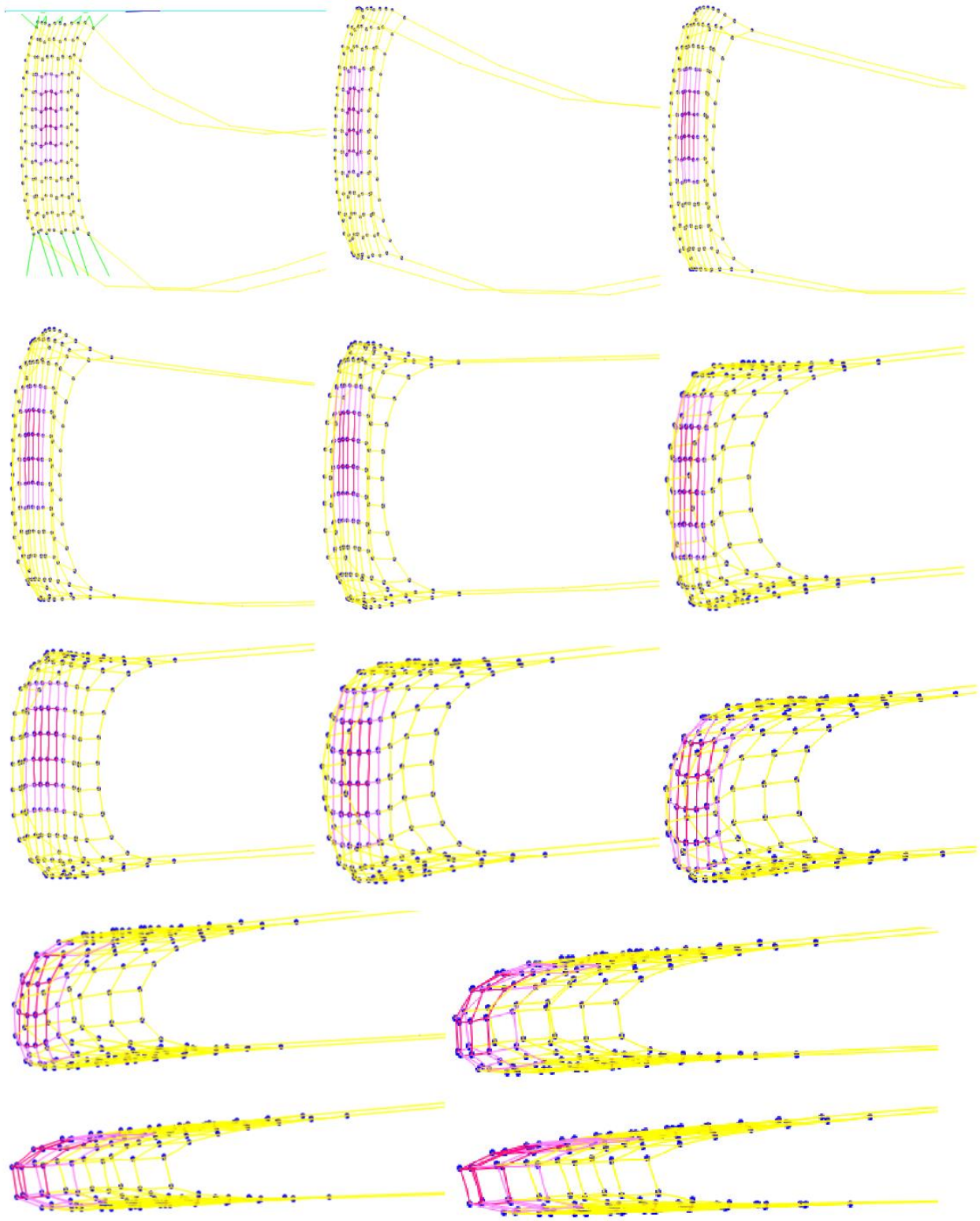

Figure 36. *Cont*.

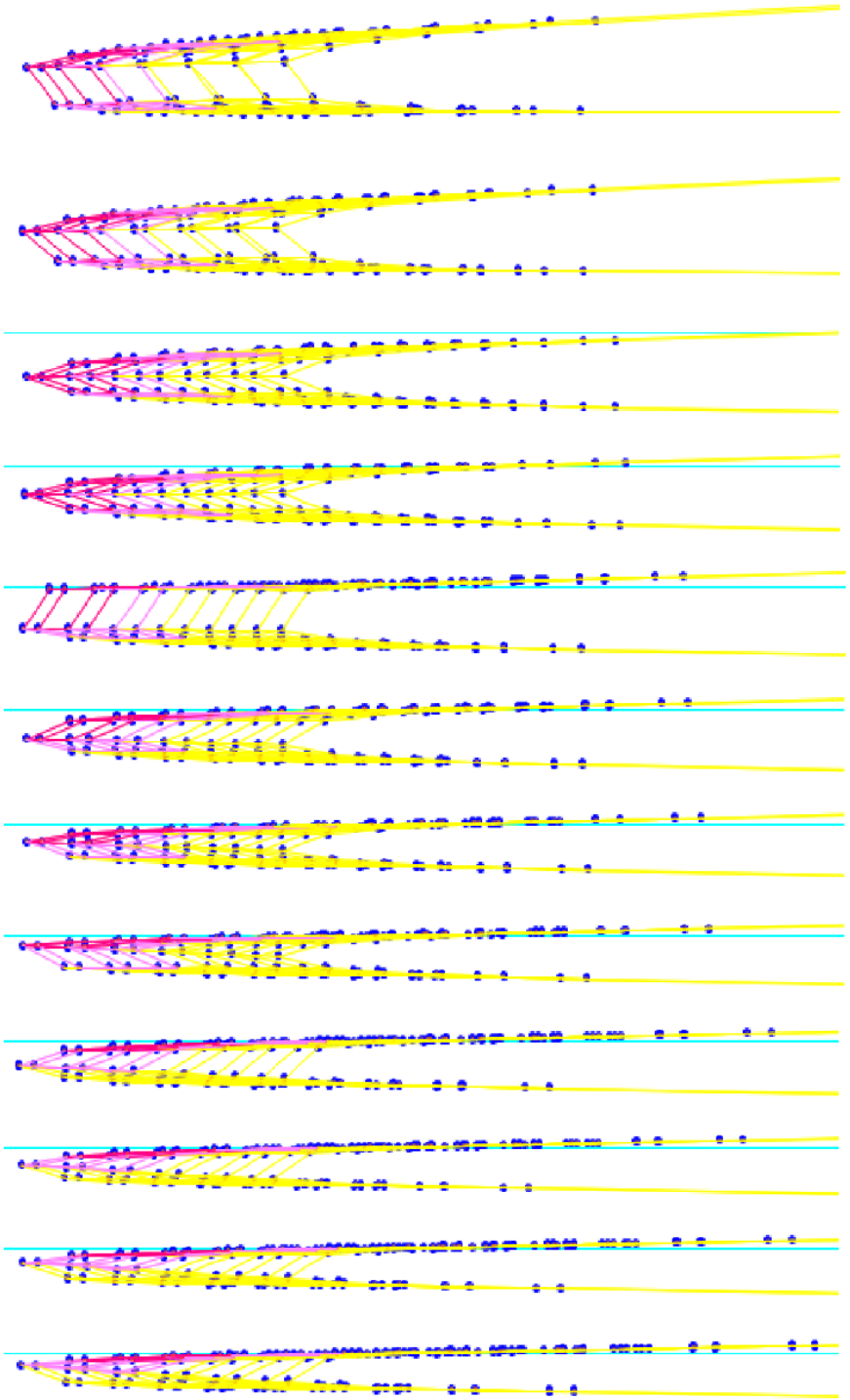

Figure 36. Shape changes of the flexible trawl in straight-line towing at v = 5 m/s.

From Figures 32–36 it can be found that, when encountering the current flow, the shape of the flexible trawl changes from a large opening to a small opening. At the beginning, the shape of the center of the trawl remains unchanged. The first structure to change is the trawl ends connected to the cable. During towing, the mesh port slowly shrinks and converges toward the center. The greater the drag speed, the faster the mesh opening shrinks. To summarize, for the flexible trawling system, the change of the towing speed of the trawler will not affect the final shape of the trawl, but it will affect the stability of the cable tension. It is easier for the cable tension to achieve stability at a low towing speed. The towing speed of the trawler should be reduced as much as possible in terms of improving

the stability of the cable tension. Moreover, once the cable in the state of rapid growth is broken, high-speed rebound will occur. The rapid rebound degree will be far greater than the rebound caused by the sudden break of the cable in the tension stabilization stage. The damage caused by this high-speed rebound to the equipment at the tail of the trawler is incalculable, and it also poses a serious threat to the life safety of the staff waiting for the recovery of the trawl at the tail of the trawler.

5. Conclusions

In this paper, the dynamic characteristics of a rigid truss trawl system and a flexible trawl system are investigated. The effects of towing speeds on the dynamic responses of the truss trawl systems during straight-line towing and rotation towing are studied using the numerical method. This research demonstrated the following:

(1) During straight-line towing, the higher the speed, the greater the tension of the cable. The tension makes the cable straighten in the axial direction. Therefore, the bending deformation of the cable is very weak in straight-line towing. Due to the rigid truss, the shape of the trawl under different towing speeds is not much different.
(2) During rotating towing, the tension of the cable changes abruptly in the initial stage, and then fluctuates periodically in the time domain. With the increase of towing speed, the overall outward floating distance of the trawl increases gradually. The change rate of the turning angle in the horizontal plane also increases, which leads to the increase of the outward floating distance of the trawl.
(3) The change of the towing speed of the trawler will not affect the final shape of the trawl, but it will affect the stability of the cable tension. It is easier for the cable tension to achieve stability at a low towing speed. The towing speed of the trawler should be reduced as much as possible in terms of improving the stability of the cable tension.

The main deficiency of this paper is the lack of corresponding model test verification. Subsequent research will focus on the establishment of model tests and further verification of mathematical models.

Author Contributions: Conceptualization, D.Z. and B.Z; methodology, D.Z. and H.J.; software, K.Z.; validation, D.Z. and K.Z.; formal analysis, D.Z. and B.Z; investigation, K.Z. and B.Z.; resources, D.Z.; data curation, K.Z.; writing—original draft preparation, D.Z.; writing—review and editing, D.Z.; visualization, K.Z.; supervision, D.Z. and H.J.; funding acquisition, D.Z. and H.J. All authors have read and agreed to the published version of the manuscript.

Funding: This research was funded by the Program for Scientific Research Start-up Funds of Guangdong Ocean University, grant number 060302072101, and Zhanjiang Marine Youth Talent Project—Comparative Study and Optimization of Horizontal Lifting of Subsea Pipeline, grant number 2021E5011, and the National Natural Science Foundation of China, grant number 62272109.

Institutional Review Board Statement: Not applicable.

Informed Consent Statement: Not applicable.

Data Availability Statement: Not applicable.

Conflicts of Interest: The authors declare no conflict of interest.

References

1. Atkinson, A.; Siegel, V.; Pakhomov, E.A.; Jessopp, M.J.; Loeb, V. A re-appraisal of the total biomass and annual production of Antarctic krill. *Deep. Sea Res. Part I Oceanogr. Res. Pap.* **2009**, *56*, 727–740. [CrossRef]
2. Nicol, S.; Foster, J.; Kawaguchi, S. The fishery for Antarctic krill–recent developments. *Fish Fish.* **2012**, *13*, 30–40. [CrossRef]
3. Cashion, T.; Al-Abdulrazzak, D.; Belhabib, D.; Derrick, B.; Divovich, E.; Moutopoulos, D.K.; Noël, S.; Palomares, M.L.D.; Teh, L.C.; Zeller, D. Reconstructing global marine fishing gear use: Catches and landed values by gear type and sector. *Fish. Res.* **2018**, *206*, 57–64. [CrossRef]
4. Park, H.; Cho, B.; Ko, G.; Chang, H. The gear shape and cross section of sweep at mouth of a bottom trawl. *J. Korean Soc. Fish. Ocean Technol.* **2008**, *44*, 120–128. [CrossRef]

5. Sala, A.; Lucchetti, A.; Palumbo, V.; Hansen, K. Energy saving trawl in Mediterranean demersal fisheries. In *Maritime Industry, Ocean Engineering and Coastal Resources*; Taylor & Francis Group: London, UK, 2008; pp. 961–964.
6. Tang, M.; Dong, G.; Xu, T.; Zhao, Y.; Bi, C. Numerical simulation of the drag force on the trawl net. *Turk. J. Fish. Aquat. Sci.* **2017**, *17*, 1219–1230.
7. Li, L.Z.; Chen, S.; Yang, J.L.; Liu, J.; Wu, Y.; Qu, T.C.; Rao, X.; Huang, H.L. Performance analysis of the four-panel mid-water trawl for Antarctic krill fishery. *J. Fish. Sci. China* **2017**, *24*, 893–901.
8. Wileman, D.A.; Hansen, K. *Estimation of the Drag of Trawls of Known Geometry*; Danish Fisheries Technology Institute: Hirtshals, Denmark, 1988.
9. Somerton, D.A.; Munro, P.T.; Weinberg, K.L. Whole-gear efficiency of a benthic survey trawl for flatfish. *Fish. Bull.* **2007**, *105*, 278–291.
10. Priour, D. FEM modeling of flexible structures made of cables, bars and nets. In *Maritime Transportation and Exploitation of Ocean and Coastal Resources*; Taylor & Francis Group: London, UK, 2005; pp. 1285–1292.
11. Mulvany, N.; Tu, J.Y.; Chen, L.; Anderson, B. Assessment of two-equation turbulence modelling for high Reynolds number hydrofoil flows. *Int. J. Numer. Methods Fluids* **2004**, *45*, 275–299. [CrossRef]
12. Kristiansen, T.; Faltinsen, O.M. Modelling of current loads on aquaculture net cages. *J. Fluids Struct.* **2012**, *34*, 218–235. [CrossRef]
13. Khaled, R.; Priour, D.; Billard, J. Numerical optimization of trawl energy efficiency taking into account fish distribution. *Ocean Eng.* **2012**, *54*, 34–45. [CrossRef]
14. Khaled, R.; Priour, D.; Billard, J. Cable length optimization for trawl fuel consumption reduction. *Ocean Eng.* **2013**, *58*, 167–179. [CrossRef]
15. Lee, J.; Yoon, H.; Park, Y.; Choi, K.; Lee, C.; Shim, D.; Park, S. Design and fabrication of fluid flow characteristic controllable trawl door using a trailing edge flap. *J. Mech. Sci. Technol.* **2019**, *33*, 5623–5630. [CrossRef]
16. Thierry, N.N.B.; Tang, H.; Achile, N.P.; Xu, L.; Hu, F.; You, X. Comparative study on the full-scale prediction performance of four trawl nets used in the coastal bottom trawl fishery by flume tank experimental investigation. *Appl. Ocean Res.* **2020**, *95*, 102022. [CrossRef]
17. Thierry, N.N.B.; Tang, H.; Liuxiong, X.; You, X.; Hu, F.; Achile, N.P.; Kindong, R. Hydrodynamic performance of bottom trawls with different materials, mesh sizes, and twine thicknesses. *Fish. Res.* **2020**, *221*, 105403. [CrossRef]
18. You, X.; Hu, F.; Takahashi, Y.; Shiode, D.; Dong, S. Resistance performance and fluid-flow investigation of trawl plane netting at small angles of attack. *Ocean Eng.* **2021**, *236*, 109525. [CrossRef]
19. Wan, R.; Jia, M.; Guan, Q.; Huang, L.; Cheng, H.; Zhao, F.; He, P.; Hu, F. Hydrodynamic performance of a newly-designed Antarctic krill trawl using numerical simulation and physical modeling methods. *Ocean Eng.* **2019**, *179*, 173–179. [CrossRef]
20. Wan, R.; Guan, Q.; Huang, L.; Li, Z.; Zhou, C.; Wang, L.; Jia, M. Effects of otter board and cable length on hydrodynamic performance of Antarctic krill trawl system. *Ocean Eng.* **2021**, *236*, 109408. [CrossRef]
21. Chen, Y.; Yao, Y. Numerical modelling of trawl net considering fluid-structure interaction based on hybrid volume method. *Turk. J. Fish. Aquat. Sci.* **2019**, *20*, 39–50.
22. Guan, Q.; Zhu, W.; Zhou, A.; Wang, Y.; Tang, W.; Wan, R. Numerical and Experimental Investigations on Hydrodynamic Performance of a Newly Designed Deep Bottom Trawl. *Front. Mar. Sci.* **2022**, *9*, 891046. [CrossRef]
23. Nyatchouba Nsangue, B.T.; Tang, H.; Xu, L.; Hu, F.; Dong, S.; Achille, N.P.; Zou, B. Comparison between physical model testing and numerical simulation using two-way fluid-structure interaction approach of new trawl design for coastal bottom trawl net. *Ocean Eng.* **2021**, *233*, 109112. [CrossRef]
24. Martin, T.; Kamath, A.; Wang, G.; Bihs, H. Modelling Open Ocean Aquaculture Structures Using CFD and a Simulation-Based Screen Force Model. *J. Mar. Sci. Eng.* **2022**, *10*, 332. [CrossRef]
25. Vu, M.T.; Van, M.; Bui, D.H.P.; Do, Q.T.; Huynh, T.; Lee, S.; Choi, H. Study on dynamic behavior of unmanned surface vehicle-linked unmanned underwater vehicle system for underwater exploration. *Sensors* **2020**, *20*, 1329. [CrossRef]
26. Vu, M.T.; Choi, H.; Kang, J.; Ji, D.; Jeong, S. A study on hovering motion of the underwater vehicle with umbilical cable. *Ocean Eng.* **2017**, *135*, 137–157.
27. Vu, M.T.; Choi, H.; Nhat, T.Q.M.; Nguyen, N.D.; Lee, S.; Le, T.; Sur, J. Docking assessment algorithm for autonomous underwater vehicles. *Appl. Ocean Res.* **2020**, *100*, 102180. [CrossRef]
28. Vu, M.T.; Choi, H.; Nguyen, N.D.; Kim, S. Analytical design of an underwater construction robot on the slope with an up-cutting mode operation of a cutter bar. *Appl. Ocean Res.* **2019**, *86*, 289–309. [CrossRef]
29. Vu, M.T.; Jeong, S.; Choi, H.; Oh, J.; Ji, D. Study on down-cutting ladder trencher of an underwater construction robot for seabed application. *Appl. Ocean Res.* **2018**, *71*, 90–104. [CrossRef]
30. Vu, M.T.; Choi, H.; Kim, J.; Tran, N.H. A study on an underwater tracked vehicle with a ladder trencher. *Ocean Eng.* **2016**, *127*, 90–102. [CrossRef]
31. Zhang, D.; Yan, J.; Zhu, K. Hydrodynamic characteristics of deep sea station cage under different failure modes of mooring cables. *J. Guangdong Ocean Univ.* **2022**, *42*, 107–116.
32. Zhang, D.; Bai, Y.; Soares, C.G. Dynamic analysis of an array of semi-rigid "sea station" fish cages subjected to waves. *Aquac. Eng.* **2021**, *94*, 102172. [CrossRef]
33. Sen, D. A study on sensitivity of maneuverability performance on the hydrodynamic coefficients for submerged bodies. *J. Ship Res.* **2000**, *44*, 186–196. [CrossRef]

34. Kristiansen, D.; Faltinsen, O.M. Non-linear wave-induced motions of cylindrical-shaped floaters of fish farms. *Proc. Inst. Mech. Eng. Part M J. Eng. Marit. Environ.* **2009**, *223*, 361–375. [CrossRef]
35. Orcina. OrcaFlex Manual 2015. Available online: http://www.orcina.com/SoftwareProducts/OrcaFlex/Validation/index/.pdf (accessed on 1 January 2015).
36. Suzuki, K.; Takagi, T.; Shimizu, T.; Hiraishi, T.; Yamamoto, K.; Nashimoto, K. Validity and visualization of a numerical model used to determine dynamic configurations of fishing nets. *Fish. Sci.* **2003**, *69*, 695–705. [CrossRef]